Biochemistry

 Volume 38, Number 37 September 14, 1999

*Articles*

# Role of D1-His190 in the Proton-Coupled Oxidation of Tyrosine $Y_Z$ in Manganese-Depleted Photosystem II[†]

Anna-Maria A. Hays,[‡] Ilya R. Vassiliev,[§] John H. Golbeck,[§] and Richard J. Debus*,[‡]

*Department of Biochemistry, University of California at Riverside, Riverside California 92521-0129, Department of Biochemistry and Molecular Biology, The Pennsylvania State University, University Park, PA 16802*

*Received March 29, 1999; Revised Manuscript Received June 2, 1999*

ABSTRACT: To further characterize the role of D1-His190 in the oxidation of tyrosine $Y_Z$ in photosystem II, the pH dependence of $P_{680}^{\bullet+}$ reduction was measured in H190A and Mn-depleted wild-type* PSII particles isolated from the cyanobacterium, *Synechocystis* sp. PCC 6803. Measurements were conducted in the presence and absence of imidazole and other small organic bases. In H190A PSII particles, rapid reduction of $P_{680}^{\bullet+}$ attributed to electron transfer from $Y_Z$ increased dramatically above pH 9, with an apparent p$K_A$ of ~10.3. In the presence of ethanolamine and imidazole, this dramatic increase occurred at lower pH values, with the efficiency of $Y_Z$ oxidation correlating with the solution p$K_A$ value of the added base. We conclude that the p$K_A$ of $Y_Z$ is ~10.3 in D1-H190A PSII particles. In Mn-depleted wild-type* PSII particles, $P_{680}^{\bullet+}$ reduction was accelerated by all exogenous bases examined (substituted imidazoles, histidine, Tris, and 1,4-diazabicyclo[2.2.2]octane). We conclude that $Y_Z$ is solvent accessible in Mn-depleted wild-type* PSII particles and that its p$K_A$ is near that of tyrosine in solution. In Mn-depleted wild-type* PSII particles, over 80% of the kinetics of $P_{680}^{\bullet+}$ reduction after a flash could be described by three kinetic components. The individual rate constants of these components varied slightly with pH, but their relative proportions varied dramatically with pH, showing apparent p$K_A$ values of 7.5 and 6.25 (6.9 and 5.8 in the presence of $Ca^{2+}$ and $Mg^{2+}$ ions). An additional p$K_A$ value (p$K_A$ < 4.5) may also be present. To describe these data, we propose (1) the p$K_A$ of His190 is 6.9−7.5, depending on buffer ions, (2) the deprotonation of $Y_Z$ is facilitated by the transient formation of a either a hydrogen bond or a hydrogen-bonded water bridge between $Y_Z$ and D1-His190, and (3) when protonated, D1-His190 interacts with nearby residues having p$K_A$ values near 6 and 4. Because $Y_Z$ and D1-His190 are located near the Mn cluster, these residues may interact with the Mn cluster in the intact system.

Photosynthetic water oxidation takes place in photosystem II (PSII)[1] near the lumenal surface of the thylakoid membrane. PSII is a multisubunit, integral membrane protein complex (*1*, *2*) that utilizes light energy to oxidize water and reduce plastoquinone (for review, see refs *3*−*10*). The oxygen-evolving catalytic site contains four Mn ions that are arranged in a multinuclear cluster. The Mn cluster accumulates oxidizing equivalents in response to photochemical events within PSII, then catalyzes the oxidation of two water molecules, releasing one molecule of $O_2$ as a

[†] This work was funded by the National Institutes of Health (GM 43496 to R.J.D.) and by the National Science Foundation (MCB 972366 to J.H.G.).

* To whom correspondence should be addressed. Phone: (909) 787-3483. Fax: (909) 787-4434. Email: debusrj@citrus.ucr.edu.

[‡] University of California at Riverside.

[§] The Pennsylvania State University.

10.1021/bi990716a CCC: $18.00 
Published on Web 08/24/1999

byproduct. The photochemical events that precede water oxidation take place in a heterodimer of two homologous polypeptides known as D1 and D2. These events are initiated by the capture of light by an antenna complex that is located peripherally to PSII. The excitation energy is transferred to the photochemically active chlorophyll species known as $P_{680}$. Excitation of $P_{680}$ results in formation of the charge-separated state, $P_{680}^{\bullet+}Q_A^{\bullet-}$, where $Q_A$ is a molecule of plastoquinone. The $P_{680}^{\bullet+}$ radical rapidly oxidizes tyrosine $Y_Z$ (Tyr161 of the D1 polypeptide), forming the neutral radical, $Y_Z^{\bullet}$. This radical in turn oxidizes the Mn cluster, while $Q_A^{\bullet-}$ reduces the secondary plastoquinone, $Q_B$. Subsequent charge separations result in further oxidation of the Mn cluster. During each catalytic cycle, the Mn cluster cycles through five oxidation states termed $S_n$, where *n* denotes the number of oxidizing equivalents stored. The $S_1$ state predominates in dark-adapted samples. The $S_3$ state may have one oxidizing equivalent localized on a Mn ligand: whether Mn is oxidized during the $S_2 \rightarrow S_3$ transition is currently under debate (e.g., see ref *11* versus ref *12*). The $S_4$ state is a transient intermediate that reverts to the $S_0$ state with the concomitant release of $O_2$. In addition to $Y_Z$, PSII contains a second redox-active tyrosine residue, known as $Y_D$ (Tyr160 of the D2 polypeptide in the numbering system of *Synechocystis* sp. PCC 6803). This tyrosine residue is also oxidized by $P_{680}^{\bullet+}$, but its function remains unknown. $Y_Z$ and $Y_D$ appear to be located symmetrically with respect to the probable $C_2$ symmetry axis of the PSII reaction center (*13*).

Recent data show that $Y_Z$ is located close to the Mn cluster. Simulations of EPR and ENDOR data from inhibited samples trapped in the $S_2Y_Z^{\bullet}$ state has yielded a $Mn-Y_Z^{\bullet}$ point−dipole distance of ∼8 Å (*14*−*16*). This distance is consistent with a geometric center-to-center distance of ∼9 Å between $Y_Z$ and the Mn cluster and is consistent with a hydrogen bond existing between $Y_Z$ and a Mn-bound water molecule (*17*). These data, plus data showing that $Y_Z^{\bullet}$ is rotationally mobile (*18*−*20*), have led to new models for the mechanism of water oxidation in PSII. These models postulate that $Y_Z$ participates directly in water oxidation by abstracting protons (*4*, *20*) or hydrogen atoms (*17*, *19*, *21*−*25*) from water-derived ligands of the Mn cluster. Whether these abstractions occur during all of the S-state transitions (*19*, *21*−*24*), only the $S_2 \rightarrow S_3$ and $S_3 \rightarrow (S_4) \rightarrow S_0$ transitions (*4*, *17*), or only the $S_2 \rightarrow S_3$ transition (*25*) is currently under debate. In all of these models, electron transfer from $Y_Z$ to $P_{680}^{\bullet+}$ is facilitated by the deprotonation of $Y_Z$ by a nearby base. On the basis of modeling studies that place D1-His190 close to $Y_Z$ (*26*−*29*), this base has long been presumed to be D1-His190. This presumption has been supported by studies involving site-directed mutagenesis (*30*−*36*) and chemical complementation (*35*). In the latter study, we measured the rates of $Y_Z$ oxidation, $P_{680}^{\bullet+}$ reduction, and $Y_Z^{\bullet}$ reduction in PSII particles isolated from several D1-His190 mutants constructed in the cyanobacterium, *Synechocystis* sp. PCC 6803 (*35*). These rates were slowed dramatically in all mutant PSII particles examined, but were accelerated dramatically in the presence of imidazole and other small organic bases. We concluded that the oxidation of $Y_Z$ by $P_{680}^{\bullet+}$ requires the deprotonation of $Y_Z$, that D1-His190 is the proton acceptor for $Y_Z$, and that the hydroxyl proton of $Y_Z$ remains bound to D1-His190 during the lifetime of $Y_Z^{\bullet}$, thereby facilitating the reduction of $Y_Z^{\bullet}$.

In the same study (*35*), we found that imidazole also accelerated both $P_{680}^{\bullet+}$ and $Y_Z^{\bullet}$ reduction in Mn-depleted wild-type* PSII particles. On the basis of this unexpected finding, we concluded that $Y_Z$ and D1-His190 interact more weakly in the absence of the Mn cluster than in its presence (*35*). This conclusion is consistent with studies showing that electron transfer from $Y_Z$ to $P_{680}^{\bullet+}$ exhibits a much greater deuterium isotope effect in the absence of the Mn cluster (*37*−*40*) than in its presence (*38*, *39*, *41*, *42*).

The objective of the present study is to further characterize the role of D1-His190 in the proton-coupled oxidation of $Y_Z$ by $P_{680}^{\bullet+}$ in Mn-depleted PSII preparations. The information obtained should form a basis by which to compare the function of D1-His190 in intact PSII preparations. In this study, the pH dependence of $P_{680}^{\bullet+}$ reduction was measured in H190A mutant and Mn-depleted wild-type* PSII particles in the presence and absence of imidazole and other small organic bases. The results provide additional evidence that D1-His190 is the proton acceptor for $Y_Z$ and show that the interaction between D1-His190 and $Y_Z$ is disrupted in the absence of the Mn cluster. In the absence of the Mn cluster, the oxidation of $Y_Z$ either occurs as a concerted electron/proton-transfer event or is rate limited by the deprotonation of $Y_Z$. In either case, the rate-limiting step may involve the transient formation of a hydrogen bond or a hydrogen-bonded water bridge between $Y_Z$ and D1-His190. Finally, D1-His190 appears to interact with nearby residues having $pK_A$ values near 6 and 4. Because $Y_Z$ is located near the Mn cluster (*14*−*16*), these residues may ligate the Mn cluster in intact PSII preparations.

## MATERIALS AND METHODS

*Construction of Site-Directed Mutants.* The D1-H190A mutation was constructed in the *psb*A-2 gene of the cyanobacterium *Synechocystis* sp. PCC 6803. The mutation-bearing plasmid was constructed as described previously (*43*). To simplify the isolation of PSII particles, the mutation-bearing plasmid was transformed into a strain of *Synechocystis* that lacks PSI and *apc*E function (*44*). The wild-type* strain was constructed in an identical manner, but with a transforming plasmid that carried no site-directed mutation. The designation "wild-type*" differentiates this strain from the native wild-type strain that contains all three *psb*A genes, contains PSI, contains a functional *apc*E gene, and is sensitive to antibiotics. Wild-type* and D1-H190A cultures were propagated in the presence of 15 mM glucose (*45*), as described previously (*35*). The mutant D2-Y160F, described previously (*46*), was propagated in the presence of 5 mM glucose. This mutant contains PSI and a functional *apc*E gene.

[1] Abbreviations: Chl, chlorophyll *a*; $Chl_Z$, monomeric chlorophyll species that is oxidized by $P_{680}^{\bullet+}$; EPR, electron paramagnetic resonance; ENDOR, electron nuclear double resonance; fwhm, full width at half-maximum; PSII, photosystem II; $P_{680}$, chlorophyll species that serves as the light-induced electron donor in PSII; $Y_Z$, tyrosine residue that mediates electron transfer between the Mn cluster and $P_{680}^{\bullet+}$; $Y_D$, tyrosine residue known to act as an alternate electron donor to $P_{680}^{\bullet+}$; $Q_A$, primary plastoquinone electron acceptor; $Q_B$, secondary plastoquinone electron acceptor; Mes, 2-(*N*-morpholino)ethanesulfonic acid; Tes, 2-{[tris-(hydroxymethyl)methyl]amino}ethanesulfonic acid; Ches, 2-(*N*-cyclohexylamino)ethanesulfonic acid; Tris, tris-(hydroxymethyl)-aminomethane; wild-type*, control strain of *Synechocystis* sp. PCC 6803 constructed in identical fashion as the mutants, but containing the wild-type *psb*A-2 gene.

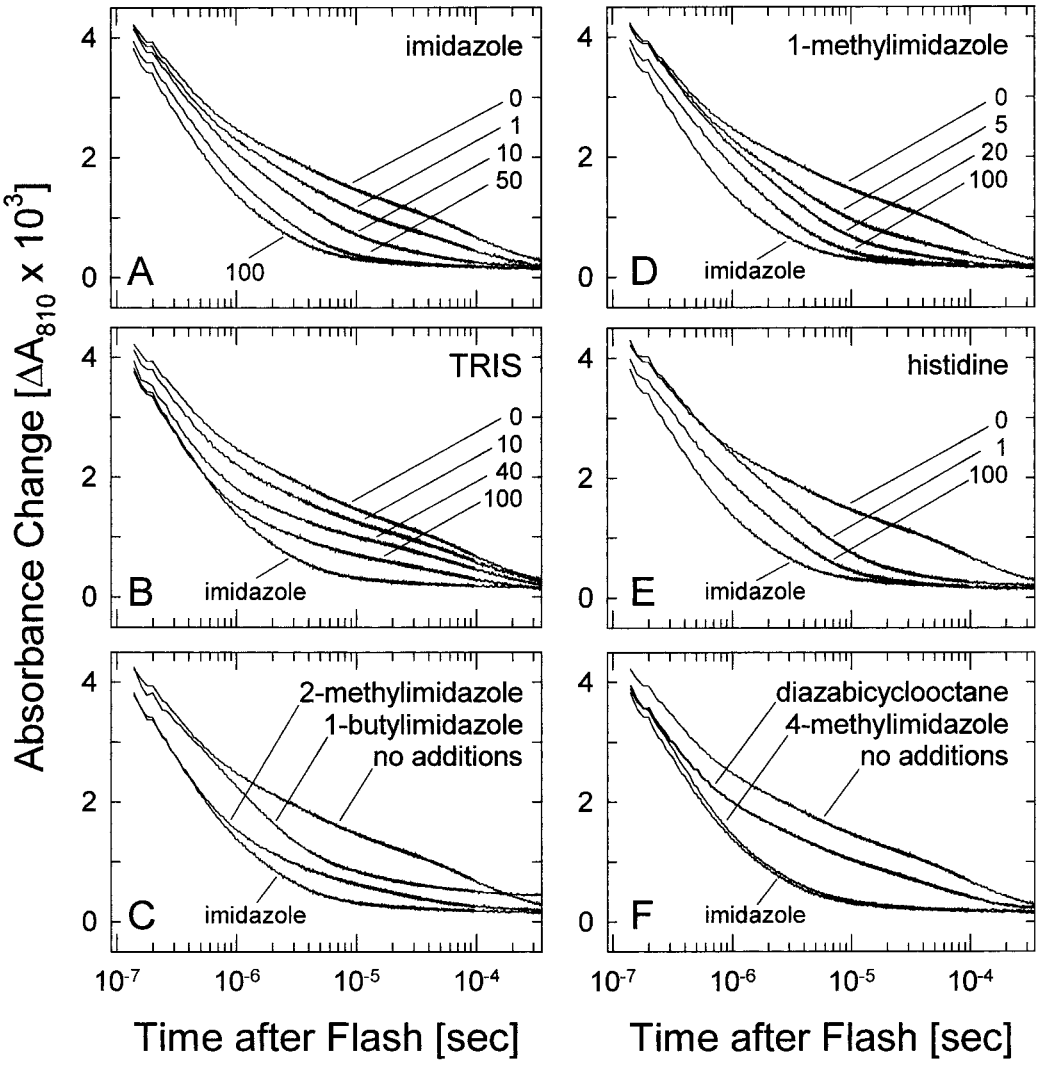


FIGURE 1: Formation and decay of $P_{680}^{\bullet+}$ in Mn-depleted wild-type* PSII particles at pH 7.5, as monitored at 810 nm: (A) in the presence of 0, 1, 10, 50, and 100 mM imidazole, (B) in the presence of 0, 10, 40, and 100 mM Tris, (C) in the presence of 100 mM 2-methylimidazole and 100 mM 1-butylimidazole, (D) in the presence of 0, 5, 20, and 100 mM 1-methylimidazole, (E) in the presence of 0, 1, and 100 mM histidine, (F) in the presence of 100 mM 1,4-diazabicyclo[2.2.2]octane and 100 mM 4-methylimidazole. The trace corresponding to 100 mM imidazole in panel A is reproduced in all other panels for comparison and is indicated by "imidazole". Conditions: 10 $\mu$g of Chl in 0.35 mL of 20 mM Tes, 0.04% *n*-dodecyl-$\beta$-D-maltoside, 10 $\mu$M $K_3Fe(CN)_6$, pH 7.5, 21 °C. Laser flashes (532 nm, 10 ns fwhm) were applied at 10 s intervals. Each trace represents the average of 8−10 sweeps.

*Isolation of PSII Particles.* Wild-type* and D1-H190A PSII particles were isolated as described previously for strains lacking PSI and *apc*E function (*35*) except that the detergent-extracted thylakoid membranes were applied to a 300 mL DEAE-Toyopearl 650s column, the column was washed with purification buffer [25% (v/v) glycerol, 50 mM Mes−NaOH, 20 mM $CaCl_2$, 5 mM $MgCl_2$, 0.03% *n*-dodecyl $\beta$-D-maltoside, pH 6.0], and the purified PSII particles were eluted with purification buffer containing 50 mM $MgSO_4$. These procedures are derived from those of Tang and Diner for isolating PSII from *Synechocystis* sp. PCC 6803 in the presence of PSI (*47*). D2-Y160F PSII particles were isolated as described by Tang and Diner (*47*), with minor modifications (*35*). Mn-depleted wild-type* and D2-Y160F PSII particles were prepared with $NH_2OH$ and EDTA, as described previously (*35*). The residual $O_2$ evolution activity of the Mn-depleted preparations was 4−6% compared to untreated wild-type* and D2-Y160F PSII particles. The H190A mutant PSII particles appeared to lack photooxidizable Mn ions and were not extracted to remove Mn. Purified and Mn-depleted PSII particles were concentrated to 0.6−0.9 mg of Chl/mL by ultrafiltration, frozen in liquid $N_2$ and stored at −80 °C. The purified PSII particles lack $Q_B$ (*47*).

*Optical Measurements.* Transient optical absorbance changes at 810 or 811 nm were measured with a laboratory-built double-beam spectrophotometer described previously (*48*). Flash excitation was provided by a frequency doubled, Q-switched DCR-11 Nd:YAG laser (Spectra-Physics) operating at 532 nm with a pulse fwhm of 10 ns and a flash energy of 22 mJ. For the experiments of Figure 1, the measuring beam (120 mW at 810 nm) was provided by a TI-SPB titanium-sapphire laser (Schwartz Electo-Optics, Orlando, FL) pumped with a diode-pumped frequency-doubled CW Nd:YAG laser, Mellenia (Spectra-Physics, Mountain View, CA) emitting at 532 nm with 5.3 mW output power. For all other experiments, the measuring beam (50 mW at 811 nm) was provided by a DC25 F semiconductor diode laser (Spindler & Hoyer, Germany). For measurements, samples were diluted (10−20 $\mu$g of Chl into 0.35 mL of final volume) into solutions containing 20 mM buffer [Mes−

NaOH(D) for pL 4.5−6.5, Tes−NaOH(D), for pL 7.0−8.5, Ches−NaOH(D) for pL 9.0−10.5], 0.04% *n*-dodecyl $\beta$-D-maltoside, and 10 $\mu$M potassium ferricyanide, plus other components (exogenous bases, $CaCl_2$, $MgCl_2$) as indicated in the figure legends. Buffers in $D_2O$ were prepared with freshly opened $D_2O$. The pL values of the buffers (L = H or D) were measured with a glass electrode calibrated with standard pH buffers and were adjusted with NaOH or freshly opened NaOD. The pD values were obtained by adding 0.40 to the meter reading (*49*, *50*). After dilution, samples were incubated in darkness for 2 min to ensure oxidation of $Q_A$ by the potassium ferricyanide and to allow equilibration with exogenous bases. Actinic flashes were applied at 0.1 Hz. To minimize denaturation of sample at extremes of pH, the entire time that elapsed between dilution of sample and completion of data acquisition was approximately 5 min. Kinetics were analyzed with Jandel Scientific's (San Rafael, CA) Peakfit Program, version 4.0.

*Other Procedures*. Chlorophyll *a* concentrations and light-saturated rates of oxygen evolution were obtained as described previously (*35*).

## RESULTS

*Reduction of $P_{680}^{\bullet+}$ in Mn-Depleted Wild-Type PSII Particles in the Presence of Exogenous Bases.* The formation and decay of $P_{680}^{\bullet+}$ can be monitored in the near-infrared, where the absorbance difference spectrum, $P_{680}^{\bullet+}$ minus $P_{680}$, has a broad positive band (*51*). We employed 810 or 811 nm for our measurements. In Figure 1, we present the flash-induced formation and decay of $P_{680}^{\bullet+}$ in Mn-depleted wild-type* PSII particles at pH 7.5. The $\Delta A_{810}$ values between 140 ns and 1 ms after the actinic flash were fit with four exponentially decaying phases[2] plus a constant offset. Fewer phases yielded residuals that were decidedly nonrandom (not shown). In the absence of exogenous bases, the $P_{680}^{\bullet+}$ reduction kinetics were as follows: 48 ± 1% with $k_1^{-1}$ = 340 ± 20 ns, 21 ± 2% with $k_2^{-1}$ = 3.4 ± 0.4 $\mu$s, 9 ± 1% with $k_3^{-1}$ = 21 ± 7 $\mu$s, 18 ± 2% with $k_4^{-1}$ = 120 ± 10 $\mu$s, and 4.2 ± 0.3% offset. All organic bases examined [imidazole (p$K_A$ 6.9), 1-methylimidazole (p$K_A$ 7.2), 2-methylimidazole (p$K_A$ 7.6), 4-methylimidazole (p$K_A$ 7.5), 1-butylimidazole, histidine (p$K_A$ 6.0), Tris (p$K_A$ 8.3), and 1,4-diazabicyclo[2.2.2]octane (p$K_A$ 8.7)] accelerated the reduction kinetics (Figure 1). In each case, the amplitudes of one or more of the more rapidly decaying phases (those with rate constants $k_1$ and $k_2$) increased at the expense of the amplitudes of one or more of the more slowly decaying phases (those with rate constants $k_3$ and $k_4$). For example, in the presence of imidazole (Figure 1A), the amplitude of $k_2$ increased (from 21 to ∼31%) at the expense of that of $k_4$ (which decreased from 18 to ∼2%). For both amplitude changes, half-saturation was achieved at ∼4 mM imidazole. In addition, over the concentration range 0−100 mM, the amplitude of $k_1$ increased gradually (to ∼58%), the amplitude of $k_3$ decreased (to ∼5%), and rate constant $k_2$ increased approximately 2-fold. Similar changes in the kinetics of $P_{680}^{\bullet+}$ reduction were observed in the presence of 1-methylimidazole (Figure 1D), except that the amplitude of $k_2$ increased to a slightly greater extent and the amplitudes of $k_1$ and $k_3$ were essentially unchanged. Similar changes were also observed in the presence of histidine (Figure 1E), except that the amplitudes of $k_2$ and $k_4$ changed with half-saturation values <1 mM and the amplitudes of $k_1$ and $k_3$ were also essentially unchanged. The presence of Tris (Figure 1B) had little effect on the amplitude of $k_2$. Instead, the decrease in the amplitude of $k_4$ (half-saturation at ∼7 mM) was mirrored by an increase in the amplitude of $k_1$. No acceleration of $P_{680}^{\bullet+}$ decay was caused by the addition of 0.1 M KCl, showing that the accelerations observed in the presence of exogenous bases were not caused by an increase in ionic strength associated with adding the bases.

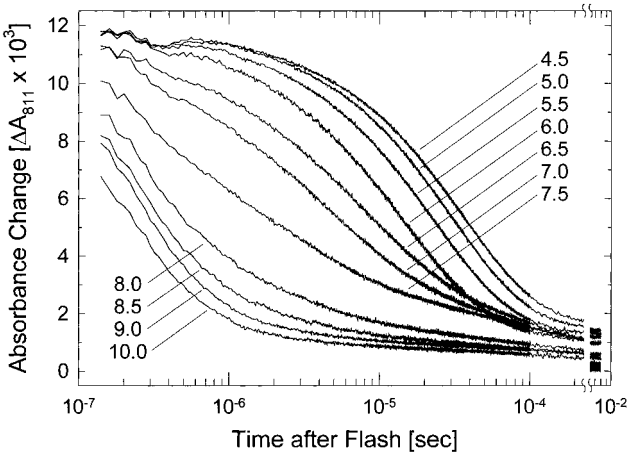


FIGURE 2: Formation and decay of $P_{680}^{\bullet+}$ in Mn-depleted wild-type* PSII particles as a function of pH, as measured at 811 nm. Conditions: same as Figure 1 except that samples contained 20 $\mu$g of Chl in 350 $\mu$L and the samples were buffered with 20 mM Mes at pH 4.5−6.5, 20 mM Tes at pH 7.0−8.5, and 20 mM Ches at pH 9.0−10.0. Laser flashes (532 nm, 10 ns fwhm) were applied at 10 s intervals. Each trace represents the average of eight sweeps. Note that the data extend over nearly 5 orders of magnitude of time.

*Reduction of $P_{680}^{\bullet+}$ in Mn-Depleted Wild-Type PSII Particles as a Function of pH*. The flash-induced formation and decay of $P_{680}^{\bullet+}$ in Mn-depleted wild-type PSII particles at pH values ranging 4.5−10 is presented in Figure 2. The rate of decay increased dramatically with pH. The $\Delta A_{811}$ values between 140 ns and 8 ms after the actinic flash were fit with five exponentially decaying phases.[2] Fewer phases yielded residuals that were decidedly nonrandom (Figure 3). Although five exponentially decaying phases were required to fit the data, the kinetics were dominated by the three fastest phases. The sum of the amplitudes of the three fastest phases varied from 77 to 85% of the total between pH 4.5 and 7.5 and exceeded 90% of the total between pH 8.0 and 10.0. The uncertainties depicted by error bars in Figures 4−6 are the sample standard deviations of the fit parameters calculated from separate measurements (e.g., three separate samples were examined at pH 7.5) or from independent fits of the same trace (e.g., at pH 4.5 and 6.5). At pH 7.5, the fits obtained were similar to those obtained from the data in

[2] The exponentially decaying phases are reported in terms of initial amplitudes (% of total) and lifetimes (i.e., $k^{-1}$), that is, the time required for the amplitude to decay to 1/*e* of its initial value. For the data presented in Figure 1, the $r^2$ values for the fits ranged 0.9962−0.9995. For the data presented in Figures 2−6, the $r^2$ values ranged 0.9918−0.9999. For the data presented in Figures 7 and 8, the $r^2$ values ranged 0.9967−0.9997.

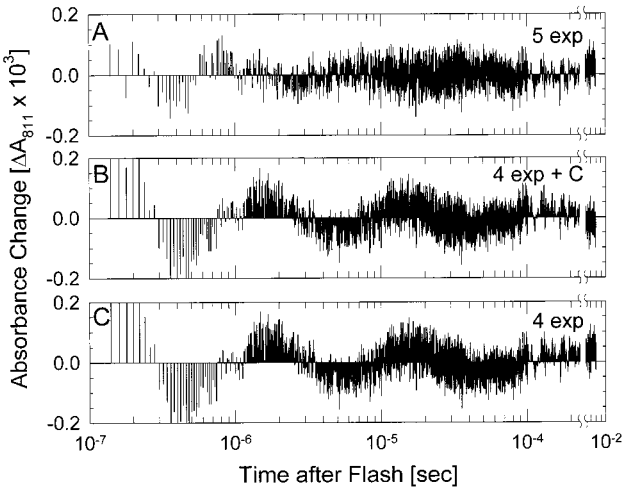


FIGURE 3: Residuals obtained from fitting the decay kinetics of $P_{680}^{\bullet+}$ in Mn-depleted wild-type* PSII particles at pH 7.5: (A) data were fit with five exponentially decaying phases, (B) data were fit with four exponentially decaying phases plus a constant offset, (C) data were fit with four exponentially decaying phases.

Figure 1 (obtained 10 months earlier);[3] at pH 7.5, the $P_{680}^{\bullet+}$ reduction kinetics were as follows: 42 ± 2% with $k_1^{-1}$ = 321 ± 27 ns, 31 ± 1% with $k_2^{-1} = 3.0 \pm 0.3$ $\mu$s, 12 ± 1% with $k_3^{-1} = 18 \pm 5$ $\mu$s, 8.9 ± 1.3% with $k_4^{-1} = 140 \pm 25$ $\mu$s, and 6 ± 1% with $k_5^{-1} = 7 \pm 2$ ms.

The amplitudes of the individual decay phases varied dramatically with pH (Figure 4). In contrast, the values of the individual rate constants varied only moderately with pH (Figure 5). For example, $k_1$ decreased only 2.8-fold between pH 10 and 7 ($k_1^{-1} \approx 0.25-0.7$ $\mu$s), $k_2$, decreased only 3.9-fold between pH 8.0 and 5.5 ($k_2^{-1} \approx 3-11$ $\mu$s), $k_3$ decreased only 2.2-fold between pH 7.5 and 5 ($k_3^{-1} \approx 20-40$ $\mu$s), and $k_4$ was largely independent of pH ($k_4^{-1} \approx 100-300$ $\mu$s at all pH values). The rate constant of the slowest phase ($k_5$) was too slow to be measured accurately because only 8 ms of data were obtained ($k_5^{-1} \approx 4-6$ ms between pH 9 and 10 and $k_5^{-1} > 6$ ms below pH 9).

The amplitude of $k_1$ increased from less than 5% to nearly 80% of the total as the pH increased, with an apparent p$K_A$ value of 7.5 (Figure 4A). The amplitude of $k_3$ decreased from over 60% to less than 4% as the pH increased, with an apparent p$K_A$ value of 6.25 (Figure 4C). The amplitude of $k_3$ may decrease below pH 5 (Figure 4C), although the precision of the data precluded a definitive statement. Nevertheless, the amplitude of $k_3$ must decrease at low pH because, at sufficiently low pH values, $Y_Z$ oxidation is blocked and $P_{680}^{\bullet+}$ is reduced by $Q_A^{\bullet-}$ (e.g., see refs *34* and *39*). The amplitude of $k_2$ was maximal near pH 6.5, decreasing at higher and lower pH values with apparent p$K_A$ values that appeared to correspond to those of $k_1$ and $k_3$ (Figure 4B). The pH profile of $k_4$ was nearly identical to that of $k_2$ (Figure 4B). Consequently, the sum of the amplitudes of $k_2$ and $k_4$ is also shown in Figure 4B.

In buffers having $D_2O$ substituted for $H_2O$, all of the apparent p$K_A$ values were increased by approximately 0.5 pH units (open circles and dashed lines in Figure 4, panels D−F). In addition, the individual rate constants decreased approximately 2-fold: the kinetic isotope effect, $k_H/k_D$, was 1.7 ± 0.2 for $k_1$, 2.5 ± 0.4 for $k_2$, and 2.6 ± 0.6 for $k_3$ (Figure 5). The increased p$K_A$ values are expected because the p$K_A$ values for weak acids, including carboxylic acids and imidazole, increase by 0.45−0.52 pH units in $D_2O$ (*52*, *53*).

The presence of 20 mM $CaCl_2$ and 5 mM $MgCl_2$ decreased the apparent p$K_A$ values of $k_1$, $k_2$, and $k_3$ by approximately 0.5 pH units (open circles and dashed lines in Figure 6, panels A−C). The values of $k_1$, $k_2$, and $k_3$ also increased, but only by factors of 1.5−1.7 (not shown).

The presence of 100 mM imidazole eliminated $k_3$ (open squares and dashed lines in Figure 6F) and $k_4$ (not shown). These observations agree with the data presented in Figure 1A, where the addition of imidazole at pH 7.5 caused $k_1$ and $k_2$ to increase at the expense of $k_3$ and $k_4$. In addition, the p$K_A$ value of $k_1$ decreased slightly, from 7.5 to ∼7.3 (Figure 6D) and the values of $k_1$ and $k_2$ increased, but only by factors of ∼1.6 (not shown).

To determine whether the absence of tyrosine $Y_D$ influences the kinetics of $P_{680}^{\bullet+}$ reduction, data were acquired with Mn-depleted PSII particles isolated from the mutant D2-Y160F. This mutant lacks $Y_D$ (*46*, *54*). The kinetics of $P_{680}^{\bullet+}$ reduction were unchanged from those shown in Figure 4, panels A−C, for wild-type* PSII particles in $H_2O$ (not shown). Therefore, we found no evidence for an influence of $Y_D$ on the reduction kinetics of $P_{680}^{\bullet+}$.

*Reduction of $P_{680}^{\bullet+}$ in D1-H190A PSII Particles as a Function of pH.* The flash-induced formation and decay of $P_{680}^{\bullet+}$ in D1-H190A PSII particles at pH values ranging 6.5−10.5 is presented in Figure 7. The rate of decay increased significantly with pH. The $\Delta A_{811}$ values between 140 ns and 8 ms after the actinic flash were fit with five exponentially decaying phases[2]. Fewer phases yielded residuals that were decidedly nonrandom (not shown). At pH 6.5, the $P_{680}^{\bullet+}$ reduction kinetics were as follows: 9 ± 1% with $k_1^{-1} = 0.7$ ± 0.2 $\mu$s, 8 ± 1% with $k_2^{-1} = 3.5 \pm 0.7$ $\mu$s, 8 ± 1% with $k_3^{-1} = 0.26 \pm 0.04$ ms, 46 ± 2% with $k_4^{-1} = 1.1 \pm 0.1$ ms, and 29 ± 2% with $k_5^{-1} = 7 \pm 1$ ms. The amplitudes of $k_1$ and $k_2$, the two phases with $k^{-1}$ values of ≤3.5 $\mu$s, increased dramatically with pH, with their sum increasing from ∼17% to over 40% with an apparent p$K_A$ value near 10 (Figure 8, filled circles and solid line). The solid line in Figure 8 represents part of a single proton titration curve extending from 17 to 83% with a p$K_A$ value of 10.3. In the presence of 100 mM ethanolamine (p$K_A$ 9.5), the apparent p$K_A$ value appeared at approximately 9.5 (Figure 8, open circles and dashed line). In the presence of 100 mM imidazole (p$K_A$ 6.9), the pH dependence of the sum of the amplitudes of $k_1$ and $k_2$ could be fit with two apparent p$K_A$ values: 6.9 and 10.3 (Figure 8, filled diamonds and dot−dashed line). This heterogeneity is presumably the result of using a subsaturating concentration of imidazole (*35*). The increases in the amplitudes of $k_1$ and $k_2$ at high pH values were accompanied by corresponding decreases in the amplitudes of $k_4$ and $k_5$. In addition, the values of $k_3$, $k_4$, and $k_5$ increased 3−4-fold over the pH range 6.5−10.5, whereas the values of $k_1$ and $k_2$ remained essentially unchanged.

We attribute the increase in the amplitudes of $k_1$ and $k_2$ above pH 9 in H190A PSII particles to the reduction of $P_{680}^{\bullet+}$ by $Y_Z$. At lower pH values, ethanolamine and imidazole

[3] When the trace at pH 7.5 was fit exactly as in Figure 1 (the $\Delta A_{811}$ values between 140 ns and 1 ms after the actinic flash fit with four exponentially decaying phases plus an offset), the $P_{680}^{\bullet+}$ reduction kinetics were as follows: 42 ± 2% with $k_1^{-1} = 325 \pm 29$ ns, 31 ± 1% with $k_2^{-1} = 3.0 \pm 0.3$ $\mu$s, 12 ± 1% with $k_3^{-1} = 18 \pm 5$ $\mu$s, 9.5 ± 1.5% with $k_4^{-1} = 150 \pm 30$ $\mu$s, and 6 ± 1% offset.

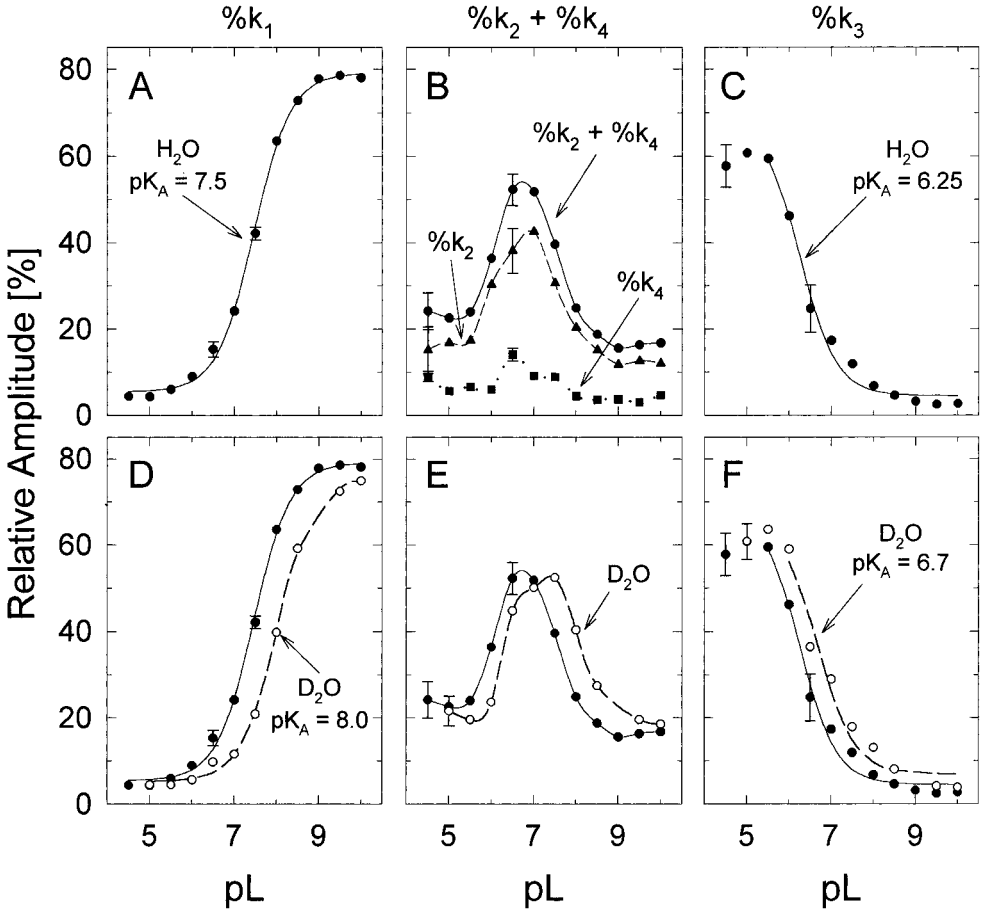


FIGURE 4: Relative amplitudes of the exponentially decaying phases of $P_{680}^{\bullet+}$ reduction in Mn-depleted wild-type* PSII particles as a function of pL: (A) % $k_1$, (B) % $k_2$ (filled triangles, dashed line), $k_4$ (filled squares, dotted line), and the sum, % $k_2$ + % $k_4$, (filled circles, solid line), (C) % $k_3$. Panels D−F compare the components measured in $D_2O$ (open circles, dashed lines) versus those measured in $H_2O$ (filled circles, solid lines, reproduced from panels A−C): (D) % $k_1$, (E) % $k_2$ + % $k_4$, (F) % $k_3$. The solid and dashed lines in panels A, C, D, and F each represent a single proton titration curve with the indicated p$K_A$ value. Conditions were the same as in Figure 2.

facilitate this reaction, presumably by facilitating the deprotonation of $Y_Z$. Note that, at pH <8 in the absence of exogenous bases, ~17% of $P_{680}^{\bullet+}$ decayed with rate constants $k_1$ or $k_2$. Similar percentages of rapidly decaying $P_{680}^{\bullet+}$ were observed in all His190 mutants examined (*35*; unpublished observations). These percentages varied with preparation. A substantial percentage (~29%) of rapidly decaying $P_{680}^{\bullet+}$ was also observed in the mutant D1-Y161F (*35*), a mutant that lacks $Y_Z$ (*55*, *56*). Consequently, we attribute the percentage of rapidly decaying $P_{680}^{\bullet+}$ observed at pH <8 in H190A, Y161F, and other His190 mutant PSII particles in the absence of exogenous bases to the reduction of $P_{680}^{\bullet+}$ by unidentified components in a percentage of PSII particles that have been structurally altered during purification.

## DISCUSSION

The oxidation of $Y_Z$ by $P_{680}^{\bullet+}$ is a proton-coupled process that can be described with the formalism shown in Figure 9. This formalism was originally developed to describe the proton-coupled reduction of $Q_B$ by $Q_A^{\bullet-}$ in bacterial reaction centers (*57*) and was first applied to PSII by Diner and coworkers (*40*). In this formalism, proton-coupled electron-transfer proceeds along one of three pathways. In the upper pathway, proton transfer to a nearby base ("B") precedes electron transfer and the tyrosinate anion is formed as an intermediate. In the lower pathway, electron-transfer precedes proton transfer and the tyrosine cation radical is formed as an intermediate. In the middle pathway, electron and proton transfer are concerted. In both upper and lower pathways, $Y_Z$ oxidation can be rate limited either by electron transfer (reactions 2 and 4) or by proton transfer (reactions 1 and 3).

The lower pathway can be excluded. First, the redox potential for generating the tyrosine cation radical is too high [$E_M \geq 1.4$ V (*58*)] to permit its formation by $P_{680}^{\bullet+}$ [$E_M \approx 1.12$ V (*59*)]. Second, the oxidation of $Y_Z$ is severely impaired in all D1-His190 mutants (*30*−*36*). In a previous study (*35*), we showed that the rate of $Y_Z$ oxidation slows dramatically in D1-His190 mutants, but is restored substantially by the addition of organic bases (*35*). In the present study, we confirm these results and show that the effectiveness of exogenous organic bases correlates with their solution p$K_A$ values (Figure 8). As in our previous study (*35*), we conclude that D1-His190 is the proton acceptor for $Y_Z$ and that the oxidation of $Y_Z$ by $P_{680}^{\bullet+}$ requires the deprotonation of $Y_Z$.

If the upper pathway applies, then whether electron or proton transfer is rate limiting can be determined from the pH dependence of the rate of $P_{680}^{\bullet+}$ reduction. If a rapid proton-transfer equilibrium precedes a rate-limiting electron transfer (reaction 2), the $P_{680}^{\bullet+}$ reduction kinetics will show

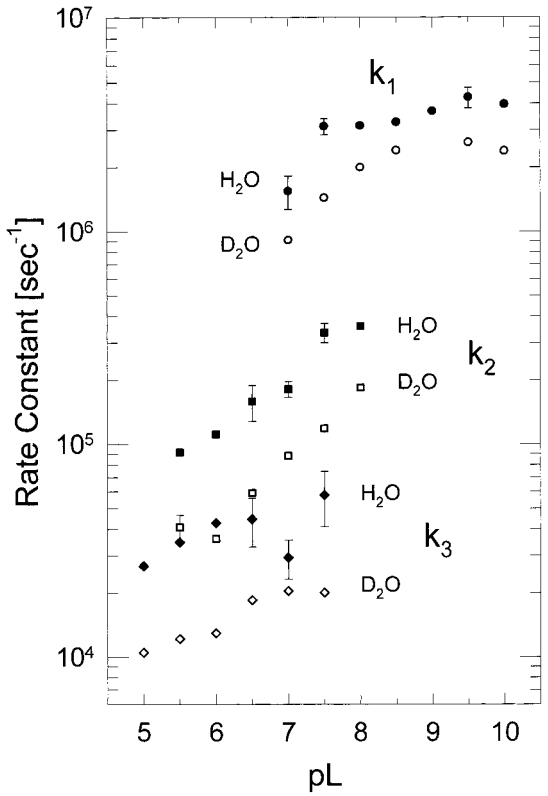


FIGURE 5: Rate constants $k_1$, $k_2$, and $k_3$ as a function of pL, measured in $H_2O$ and $D_2O$. The kinetic isotope effect, $k_H/k_D$, was $1.7 \pm 0.2$ for $k_1$, $2.5 \pm 0.4$ for $k_2$, and $2.6 \pm 0.6$ for $k_3$. Conditions were the same as in Figure 2.

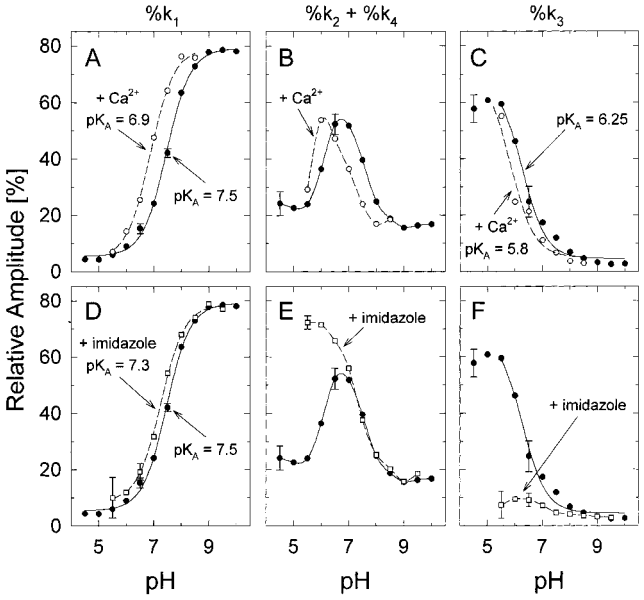


FIGURE 6: Relative amplitudes of the exponentially decaying phases of $P_{680}^{\bullet+}$ reduction in Mn-depleted wild-type* PSII particles in the presence of 20 mM $CaCl_2$ and 5 mM $MgCl_2$ (upper panels) or 100 mM imidazole (lower panels) as a function of pH: (A,D) % $k_1$, (B,E), % $k_2$ + % $k_4$, (C,F) % $k_3$. The solid or dashed lines in panels A, C, and D each represent a single proton titration curve with the indicated p$K_A$ value. Conditions were the same as in Figure 2 except that the samples also contained 20 mM $CaCl_2$ and 5 mM $MgCl_2$ (upper panels, open circles and dashed lines) or 100 mM imidazole (lower panels, open squares and dashed lines).

a pH-dependent rate constant whose value at a particular pH value will depend on the fraction of $Y_Z$ that is unprotonated at that pH value. The value of this rate constant will also

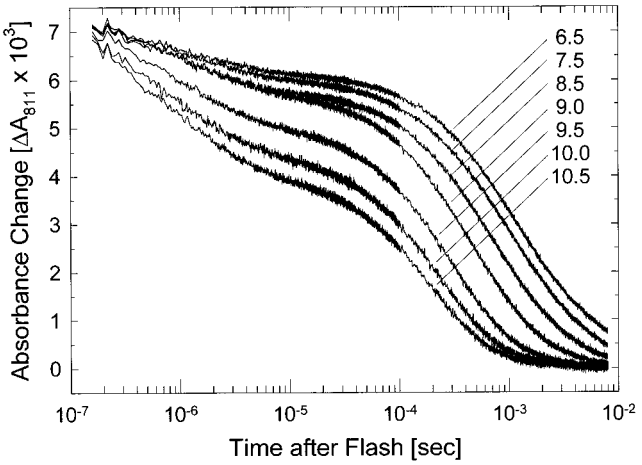


FIGURE 7: Formation and decay of $P_{680}^{\bullet+}$ in H190A PSII particles as a function of pH, as measured at 811 nm. Conditions were the same as in Figure 2 except that samples contained 15 $\mu$g of Chl in 350 $\mu$L. Note that data extend over nearly 5 orders of magnitude of time.

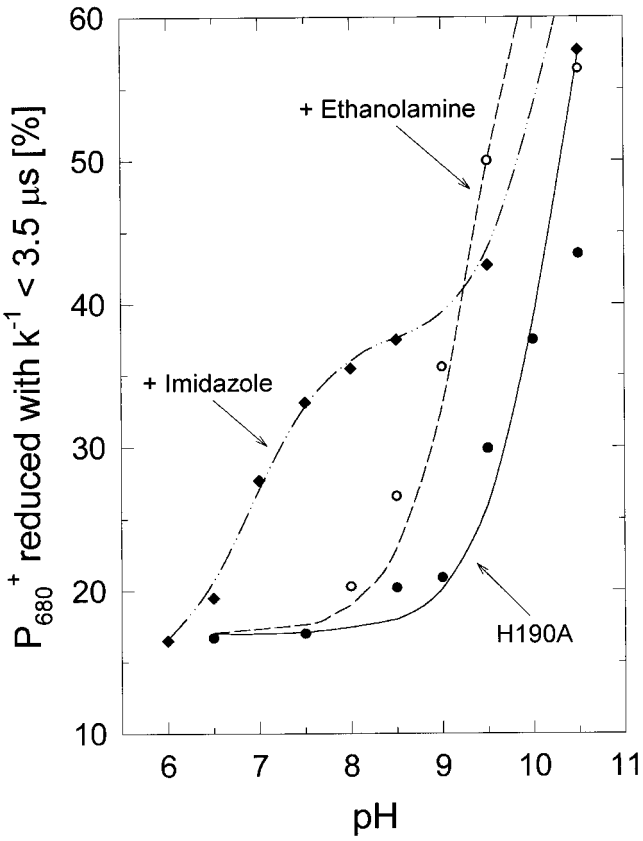


FIGURE 8: Relative amplitude of the exponentially decaying phases of $P_{680}^{\bullet+}$ reduction with $k^{-1} < 3.5$ $\mu$s in H190A PSII particles as a function of pH in the absence of exogenous bases (filled circles), in the presence of 100 mM ethanolamine (open circles) or in the presence of 100 mM imidazole (filled diamonds). The solid line represents part of a single proton titration curve (from 17 to 83%) with a p$K_A$ value of 10.3. The dashed line represents part of a single proton titration curve (from 17 to 83%) with a p$K_A$ value of 9.5. The dot−dashed line represents the sum of two titration curves, one with a p$K_A$ value of 6.9 (from 14 to 38%), and a second with a p$K_A$ value of 10.3 (from 38 to 86%). The presence of two titration curves is caused by using a sub-saturating concentration of imidazole (*35*). Conditions were the same as in Figure 7.

depend on the $\Delta G$ for the reaction. In Mn-depleted wild-type* PSII preparations, we find that the $P_{680}^{\bullet+}$ reduction

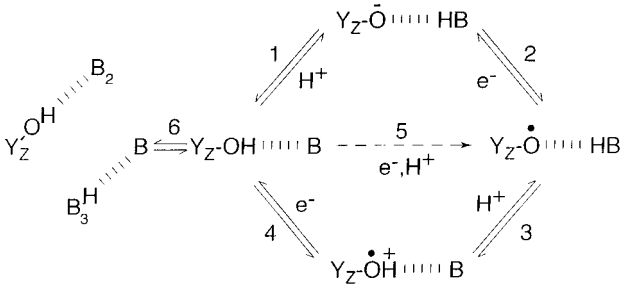


FIGURE 9: Possible reaction pathways for the proton-coupled oxidation of $Y_Z$. Base "B" denotes D1-His190. In the upper pathway, proton-transfer precedes electron transfer and the tyrosinate anion is formed as an intermediate. In the lower pathway, electron-transfer precedes proton transfer and the tyrosine cation radical is formed as an intermediate. In the middle pathway, electron and proton transfer are concerted. In both upper and lower pathways, $Y_Z$ oxidation can be rate-limited either by electron transfer (reactions 2 and 4) or by proton transfer (reactions 1 and 3). Reaction 6 represents a hypothetical equilibrium between $Y_Z$ and D1-His190 forming a hydrogen bond with each other and with other partners, e.g., the groups denoted $B_2$ and $B_3$.

kinetics are fit by multiple phases whose rate constants are relatively independent of pH (Figure 5). Furthermore, Diner and co-workers reported that the rate of electron transfer from $Y_Z$ to $P_{680}^{\bullet+}$ appears to be only weakly dependent on the $\Delta G$ for the reaction (*40*). Therefore, we conclude that, in Mn-depleted PSII preparations, either the oxidation of $Y_Z$ by $P_{680}^{\bullet+}$ is rate limited by the deprotonation of $Y_Z$ (upper pathway, reaction 1) or electron and proton transfer are concerted (middle pathway, reaction 5). Our data do not distinguish between these two possibilities.

The conclusions reached in the previous paragraph are supported by a recent study of Mn-depleted PSII particles from pea (*39*). In this study, the kinetics of $P_{680}^{\bullet+}$ reduction at pH values ranging 4−11 were fit with three exponentially decaying phases plus an offset (*39*). The two most rapidly decaying phases were attributed to $Y_Z$ oxidation. In agreement with the present study, the rate constants for these phases, $k_f$ and $k_s$, were relatively independent of pH, while their relative amplitudes varied dramatically with pH (*39*). Both $k_f$ and $k_s$ (*39*) are smaller than $k_1$ and $k_2$ (this study) by factors of ∼5 and 2−4, respectively. In addition, the deuterium isotope effect for $k_f$ was much smaller ($k_H/k_D \leq 1.1$) than measured for $k_1$ in this study ($k_H/k_D = 1.7 \pm 0.2$). In contrast, the deuterium isotope effect for $k_s$ ($k_H/k_D \approx 2.5$) was the same as that measured for $k_2$ and $k_3$ in this study ($k_H/k_D = 2.5 \pm 0.4$ and $2.6 \pm 0.6$, respectively). The discrepancies may reflect differences between *Synechocystis* and pea.

Before considering the mechanism of $Y_Z$ oxidation further, we turn to estimations of the p$K_A$ values of $Y_Z$ and D1-His190.

*Estimations of p$K_A$ Values. (1) p$K_A$ Value of $Y_Z$ in D1-H190A PSII Preparations*. The percentage of D1-H190A PSII particles having $P_{680}^{\bullet+}$ reduced rapidly (with $k^{-1} \leq 3.5$ $\mu$s) increased dramatically above pH 9 with an apparent p$K_A$ value of ∼10.3 (Figure 8). In the presence of ethanolamine or imidazole, this dramatic increase in $Y_Z$ oxidation appeared at substantially lower pH values, with the efficiency of $Y_Z$ oxidation correlating with the solution p$K_A$ value of the added base. These data show that the oxidation of $Y_Z$ by $P_{680}^{\bullet+}$ requires the deprotonation of $Y_Z$. In the absence of D1-His190, this deprotonation can be achieved by adding small organic bases or by raising the pH. We conclude that $Y_Z$ has p$K_A \approx 10.3$ in H190A PSII particles.

Our conclusion that $Y_Z$ has p$K_A \approx 10.3$ in D1-H190A PSII particles conflicts with a recent report that $Y_Z$ has p$K_A \approx$ 8.1 in thylakoid membranes isolated from dark-grown[4] cells of the *Chlamydomonas reinhardtii* mutants D1-H190F and D1-H190Y (*34*). However, we believe that the value of 8.1 reported in this study is too low. At pH 9.5, the highest pH value examined, a single saturating flash applied to H190F and H190Y thylakoid membranes produced less than 50 and 60%, respectively, of the maximum yield of variable chlorophyll *a* fluorescence (compared to ∼90% in membranes isolated from dark-grown[4] wild-type cells). In addition, a single flash applied to H190F membranes at pH 9 generated only ∼70% of an EPR transient attributed to $Y_Z^{\bullet}$ (*34*). Some of the diminished fluorescence yields at pH ≥9 in the mutant membranes might be attributed to the reduction of $P_{680}^{\bullet+}$ by $Chl_Z$ rather than by $Y_Z$ in reaction centers containing oxidized cytochrome $b_{559}$. Because $Chl_Z^{\bullet+}$ is a potent quencher of chlorophyll *a* fluorescence in PSII membranes (*60*, *61*), it could significantly quench the fluorescence yield even when present in quantities that escape detection by transient EPR experiments. On the basis of these considerations, we believe that the data in ref *34* are more consistent with a $Y_Z$ having a p$K_A$ value closer to 9 than 8. The remaining differences between the data reported in ref *34* and in the present study are not understood, although different mutants and organisms were employed in the two studies.

*(2) p$K_A$ Value of $Y_Z$ in Mn-Depleted Wild-Type* PSII Preparations*. The three dominant phases of $P_{680}^{\bullet+}$ reduction in Mn-depleted wild-type* PSII particles, $k_1$, $k_2$, and $k_3$, were relatively independent of pH and showed deuterium isotope effects, $k_H/k_D$, of 1.7−2.6 (Figure 5). Because the values of $k_H/k_D$ were independent of pH up to the highest pH value examined (pH 10), we conclude that the deprotonation of $Y_Z$ is required for its oxidation at pH <10. Therefore, we propose that $Y_Z$ has the same p$K_A$ value in Mn-depleted wild-type* PSII particles as in D1-H190A PSII particles (p$K_A \approx$ 10.3), a value close to that of tyrosine in solution. A p$K_A$ value close to that of tyrosine in solution suggests that, in Mn-depleted wild-type* PSII preparations, $Y_Z$ is readily accessible to solvent. Such facile solvent accessibility would be consistent with our observation that exogenous bases substantially accelerate $P_{680}^{\bullet+}$ reduction in Mn-depleted wild-type* PSII particles (Figure 1). Facile solvent accessibility to $Y_Z$ in the absence of the Mn cluster is also consistent with previous studies of Mn-depleted PSII preparations showing that $D_2O$ rapidly exchanges into the environment of $Y_Z$ ($t_{1/2} < 1-2$ min) (*39*, *40*), that exogenous reductants rapidly reduce $Y_Z^{\bullet}$ ($k = 10^5 - 10^7$ $M^{-1}$ $s^{-1}$) (*62*−*65*), and that, in $D_2O$ buffers, multiple deuterons exchange into the environment of $Y_Z^{\bullet}$ (*40*, *66*).

Our conclusion that $Y_Z$ has p$K_A \approx 10.3$ in Mn-depleted wild-type* PSII particles conflicts with UV difference spectra recorded at pH 9 and pH 6.1 in Mn-depleted PSII particles of *Synechocystis* sp. PCC 6803 that lack $Y_D$ (*40*). By comparing the double difference spectrum, $(Y_Z^{\bullet} - Y_Z)_{pH9}$

[4] Propagation of *C. reinhardtii* cells in total darkness prevents assembly and photoactivation of the Mn cluster (*34*).

$-(Y_Z^{\bullet} - Y_Z)_{pH6.1}$, with the spectra of tyrosine in water at pH 12 and 7.4, the authors of ref *40* concluded that ~60% of $Y_Z$ is in the tyrosinate form at pH 9. This corresponds to a p$K_A \approx 8.6$. However, this analysis relies on assuming that the extinction coefficients for tyrosine and tyrosinate in PSII are the same as in water and that the spectrum of $Y_Z^{\bullet}$ is independent of pH.

*(3) p$K_A$ Value of D1-His190 in Mn-Depleted Wild-Type* PSII Preparations*. The amplitude of the most rapid phase of $P_{680}^{\bullet+}$ reduction in Mn-depleted wild-type* PSII particles, $k_1$, increased dramatically with pH, showing an apparent p$K_A$ value of 7.5 (Figure 4A). We propose that this is the p$K_A$ of D1-His190 and that $k_1$ represents the oxidation of $Y_Z$ in the presence of an unprotonated D1-His190. A p$K_A$ value of 7.5 is greater than that of histidine in solution (p$K_A$ 6.0). The higher value in vivo could be caused by a hydrogen bond between the $\delta$1 nitrogen of D1-His190 and a nearby carboxylate residue. In many proteins, the basicity of the $\epsilon$2 nitrogen of a histidine residue is increased by a hydrogen bond between the $\delta$1 nitrogen and an Asp or Glu residue. Examples are myogloblin (*67*), T4 lysozyme (*68*), the serine proteases (*69*, *70*), and various metalloenzymes (*71*, *72*). Alternatively, the higher p$K_A$ value could be caused by an electrostatic interaction (*73*−*75*) between D1-His190 and nearby carboxylate residues that may ligate the Mn cluster in intact PSII preparations. Partial screening of these electrostatic interactions could account for the shift of the apparent p$K_A$ values of $k_1$, $k_2$, and $k_3$ in the presence of $Ca^{2+}$ and $Mg^{2+}$ ions (Figure 6, panels A−C). In any event, a p$K_A$ value of 7.5 is not far from p$K_A$ values often found for histidine residues in proteins (*76*).

An alternative assignment is that $Y_Z$ has a p$K_A \approx 7.5$ (see the discussions in refs *39*, *40*, and *77*). Such a low p$K_A$ value for tyrosine in proteins would not be unprecedented: in the H64Y mutants of sperm whale and horse heart myoglobin, Tyr64 ligates the heme and has a p$K_A$ value of 5.6 (*78*) and 4.7 (*79*), respectively. These low p$K_A$ values have been attributed to stabilization of the phenolate ion by a nearby Arg residue and by the positively charged heme iron (*78*). However, no such charged groups are located near $Y_Z$ in recent structural models of PSII (*26*−*29*). Furthermore, if a low p$K_A$ value for $Y_Z$ was caused by an intermittent interaction between $Y_Z$ and D1-His190, as proposed in refs *40* and *77*, then exogenous organic bases should lower the p$K_A$ value further. In contrast, the p$K_A$ value of 7.5 changed only slightly in the presence of 100 mM imidazole (Figure 6D), a concentration far above that required to accelerate $P_{680}^{\bullet+}$ reduction (Figure 1A). A p$K_A$ of 7.5 for $Y_Z$ would also conflict with our observation that both $k_1$ and $k_2$ show deuterium isotope effects above pH 7.5 (Figure 5). No deuterium isotope effect would be expected if $Y_Z$ is deprotonated prior to the actinic flash.

The p$K_A$ value of 7.5 reported in this study agrees favorably with values reported previously. Styring and co-workers recently determined a p$K_A$ value of 7.6 in thylakoid membranes isolated from dark-grown[4] wild-type cells of *Chlamydomonas reinhardtii* and attributed it to D1-His190 (*34*). This p$K_A$ value was obtained from measurements of the flash-induced yield of chlorophyll *a* fluorescence. The measurements were performed in the absence of added $Ca^{2+}$ and $Mg^{2+}$ ions, conditions similar to those employed in Figure 4 of the present study. Junge and co-workers recently determined a p$K_A$ value of 7.0 in Mn-depleted PSII particles isolated from pea (*39*). This value was obtained from measurements of $P_{680}^{\bullet+}$ reduction at 827 nm. The measurements were performed in the presence of 5 mM $CaCl_2$ and 5 mM $MgCl_2$. We obtained a similar value of 6.9 in the presence of 20 mM $CaCl_2$ and 5 mM $MgCl_2$ (Figure 6A). As mentioned earlier, the lower p$K_A$ value obtained in the presence of $Ca^{2+}$ and $Mg^{2+}$ ions may be caused by partial screening of electrostatic interactions between D1-His190 and nearby carboxylate residues.

Our p$K_A$ value of 7.5 contrasts with that of Diner and co-workers, who recently estimated a p$K_A$ value of 8.3 in Mn-depleted PSII particles from *Synechocystis* sp. PCC 6803 (*40*). The difference between these estimated p$K_A$ values was not caused by the absence of $Y_D$ in the previous study (*40*): we found no difference between the pH dependence of $P_{680}^{\bullet+}$ reduction in Mn-depleted PSII particles isolated from wild-type* cells or from D2-Y160F cells, which lack $Y_D$. The difference also was not caused by the presence or absence of $Ca^{2+}$ ions because neither the previous data (*40*) nor ours (Figure 2) was acquired in the presence of added $Ca^{2+}$ ions. However, an important difference between the two studies is the method of data acquisition. In ref *40*, the actinic flash had a pulse fwhm of ~1 $\mu$s. The data were acquired at discrete time points after the flash (at 1, 2, 3, 4, 6, 9, 12, 15, 20, 30, 40, 70, 95, 145, 195, and 295 $\mu$s) and were fit with two exponentially decaying phases. To approximate this method of data acquisition and analysis, we extracted 17 $\Delta A_{811}$ values from each trace in Figure 2 (the value at 160 ns after the flash plus that at each time point listed above), then fit these values with two exponentially decaying phases. The resulting analyses were similar to those presented in the previous study (*40*): the amplitude of the most rapidly decaying phase was >70% of the total amplitude at all pH values, the rate constant of this phase increased with pH with an apparent p$K_A$ value of 8.0 (compared to 8.3 in ref *40*), the apparent p$K_A$ value shifted to 8.3 in the presence of $D_2O$ (compared to 8.7 in ref *40*), and the magnitude of the deuterium isotope effect, $k_H/k_D$, showed the same dependence on pL and could be fit with the same p$K_A$ values (8.0 in $H_2O$ and 8.55 in $D_2O$) as in ref *40* (not shown). We conclude that, because of the lower time resolution available to the authors of ref *40*, the relatively pH-independent kinetic phases, $k_1$, $k_2$, and $k_3$, were convoluted into a single kinetic phase that had a large apparent pH dependence. We believe that our analysis (and our p$K_A$ value of 7.5) is more accurate than that in ref *40* because the higher time resolution of our measurements permitted the resolution of additional kinetic phases.

*Mechanism of $Y_Z$ Oxidation. (1) Oxidation of $Y_Z$ in $O_2$-Evolving Wild-Type* PSII.* In intact wild-type* PSII preparations, the kinetics of $P_{680}^{\bullet+}$ reduction are multiphasic. The majority of phases have half-times of 20−40 and 100−300 ns, and the remainder have half-times of 2−5 and 20−40 $\mu$s (*38*, *39*, *41*, *42*, *80*−*86*). The nanosecond phases exhibit no deuterium isotope effect (*38*, *39*, *41*, *42*), consistent with an electron-transfer rate limitation on $Y_Z$ oxidation. The nanosecond phases have been described in terms of nonadiabatic electron transfer theory (*58*, *77*, *87*).

In intact PSII preparations, $Y_Z$ and D1-His190 are believed to interact via a strong hydrogen bond (*41*, *58*, *77*, *88*, *89*). Some authors have proposed that this bond is so strong that

$Y_Z$ is deprotonated at neutral pH values (*77*, *88*). However, this proposal conflicts with FTIR measurements showing that the $\delta$C−O−H bending mode of $Y_Z$ (1255 $cm^{-1}$) is present at pH 6.0 in PSII preparations that retain the Mn cluster (*90*, *91*). Because of proton tunneling, the rate of proton transfer in a conventional hydrogen bond is extremely rapid (picoseconds to nanoseconds), even in a hydrogen bond having a large p$K_A$ difference between hydrogen bond donor and acceptor (*92*, *93*). Therefore, even if the p$K_A$ values of $Y_Z$ and D1-His190 are 10.3 and 7.5, respectively (vide supra), the rate of proton transfer from $Y_Z$ to D1-His190 in intact PSII preparations should be much faster than the nanosecond phases of $Y_Z$ oxidation.[5] Consequently, the existence of a conventional hydrogen bond between $Y_Z$ and D1-His190 is consistent with an electron-transfer rate limitation on $Y_Z$ oxidation in intact PSII preparations. This conclusion is consistent with recent hybrid density functional calculations on a phenol-imidazole hydrogen-bonded complex (*94*). Recently, the nanosecond phases of $P_{680}^{\bullet+}$ reduction have been proposed to occur in reaction centers where the hydroxyl proton of $Y_Z$ is either rapidly delocalized after transfer to D1-His190 (*89*) or rapidly transferred from D1-His190 to the lumenal surface via one or more proton-transfer pathways (*58*). In these reaction centers, D1-His190 is unprotonated (*89*) and the amino acid residues within the proton-transfer pathways are in protonation states that are optimal for rapid proton transfer (*58*).

*(2) Oxidation of $Y_Z$ in Mn-Depleted Wild-Type* PSII.* In Mn-depleted wild-type PSII preparations, the oxidation of $Y_Z$ by $P_{680}^{\bullet+}$ is slowed 10−1000-fold compared to the nanosecond phases of $Y_Z$ oxidation in intact PSII preparations (Figure 2 and refs *35*, *37*−*40*, and *95*−*98*). In principle, the slowed rate of $Y_Z$ oxidation could be caused by an increase in the reorganization energy for electron transfer produced by the increased solvent accessibility of $Y_Z$ (*58*, *87*). However, the rate also shows a deuterium isotope effect, $k_H/k_D$, of 2−3 (Figure 4 and refs *37*−*40*) and is substantially accelerated by the addition of imidazole and other exogenous bases (Figure 1 and ref *35*). These observations show that the interaction between $Y_Z$ and D1-His190 is altered in the absence of the Mn cluster. The alteration could correspond to an elongation or angular distortion of the hydrogen bond. An elongation of a hydrogen bond between an OH group and a nitrogen atom can increase the activation energy ($\Delta G^{\ddagger}$) for proton transfer by as much as 10 kcal/mol (*93*, *99*, *100*) (also see ref *101*). If the hydrogen bond is also distorted from its optimal geometry, $\Delta G^{\ddagger}$ can be even higher (*100*−*102*). Even when proton tunneling dominates, the rate of proton transfer is exquisitely sensitive to $\Delta G^{\ddagger}$: a 5 kcal/mol increase in $\Delta G^{\ddagger}$ could slow the rate of proton tunneling by several orders of magnitude (*100*, *103*). Therefore, an elongated or angularly distorted hydrogen bond between $Y_Z$ and D1-His190 could explain the slowed oxidation of $Y_Z$ that is observed in the absence of the Mn cluster. A direct hydrogen bond between $Y_Z$ and D1-His190 in Mn-depleted wild-type* PSII preparations would be consistent with the interpretations of a recent FTIR study (*91*). The authors of this study proposed that $Y_Z$ forms a strong hydrogen bond with a neutral histidine residue in a majority of Mn-depleted reaction centers at pH 6 (*91*).

Magnetic resonance studies show that the hydrogen bonds formed by $Y_Z^{\bullet}$ in the absence of the Mn cluster are heterogeneous compared to those formed by $Y_D^{\bullet}$ (*40*, *66*, *104*−*106*). A recent FTIR study shows that this heterogeneity applies to the hydrogen bonds formed by $Y_Z$ as well (*91*). Therefore, both $Y_Z$ (*91*) and $Y_Z^{\bullet}$ (*40*, *66*) appear to have multiple hydrogen bond partners that may include water molecules or hydroxylated side chains (*40*, *66*, *91*). Nevertheless, the oxidation of $Y_Z$ requires proton transfer to D1-His190 (*30*−*36*).

As discussed above, an elongated or angularly distorted hydrogen bond between $Y_Z$ and D1-His190 could explain the characteristics of $Y_Z$ oxidation in the absence of the Mn cluster. However, recent ENDOR measurements detect no $^{15}N$ couplings between $Y_Z^{\bullet}$ and histidine in Mn-depleted PSII particles containing $^{15}N$ histidine (K. A. Campbell, R. D. Britt, and B. A. Diner, personal communication). If $Y_Z$ and D1-His190 are sufficiently close to interact via a hydrogen bond, $^{15}N$ couplings to $Y_Z^{\bullet}$ should be detected, even if no hydrogen bond exists between $Y_Z^{\bullet}$ and D1-His190. Therefore, the ENDOR data imply that no direct hydrogen bond exists between $Y_Z$ and D1-His190 in the absence of the Mn cluster, at least under the conditions of the ENDOR experiments. To account for the ENDOR data, two alternate models are considered.

In one model [model A, originally proposed by Diner and co-workers (*40*)], the interaction between $Y_Z$ and D1-His190 is heterogeneous in the absence of the Mn cluster so that, in a significant percentage of reaction centers, $Y_Z$ and D1-His190 form hydrogen bonds with other partners. In this model, the oxidation of $Y_Z$ is rate limited by the breaking of these hydrogen bonds and the transient formation of a hydrogen bond between $Y_Z$ and D1-His190 (reaction 6 of Figure 9). The other groups that donate hydrogen bonds to D1-His190 must have p$K_A$ values greater than 10.3. Otherwise, $k_1$ would increase substantially with pH because progressively fewer of these groups would be available to compete with $Y_Z$ for D1-His190. In contrast, we find that $k_1$ exhibits very little pH dependence between pH 7.5 and 10 (Figure 5). Few residues with p$K_A \geq 10.3$ are found near $Y_Z$ in recent structural models (*26*−*29*), but D1-Gln165 and peptide amide groups are possibilities. To reconcile this model with the ENDOR data cited in ref *40*, the percentage of $Y_Z$ that forms a hydrogen bond to D1-His190 must be very small at the cryogenic temperatures employed for the ENDOR experiments.

In an alternative model (model B), the distance between $Y_Z$ and D1-His190 increases substantially in the absence of the Mn cluster (to ≥5 Å) so that the hydrogen bond between these two residues is lost (Figure 10). In this model, proton transfer from $Y_Z$ to D1-His190 takes place via a hydrogen-

[5] If the p$K_A$ values of $Y_Z$ and D1-His190 are 10.3 and 7.5, respectively, then the hydrogen bond is asymmetric and $\Delta G_o = 3.75$ kcal/mol for proton transfer from $Y_Z$ to D1-His190 [$\Delta G_o = -RT \ln K$, where $K = 10^{\Delta pK_A}$ and $\Delta pK_A = (pK_{A[ACCEPTOR]} - pK_{A[DONOR]})$]. For a symmetric hydrogen bond (a hydrogen bond with no free energy difference between the minima of the donor and acceptor potential wells, i.e., with $\Delta G_o = 0$) with an activation energy ($\Delta G^{\ddagger}$) of 7 kcal/mol, proton transfer takes place in picoseconds (*92*, *93*). In a highly asymmetric hydrogen bond with $\Delta G_o = 7.5$ kcal/mol and $\Delta G^{\ddagger} = 11.5$ kcal/mol, proton transfer takes place in nanoseconds (*92*). In the latter case, proton tunneling takes place from an excited vibrational level. Note that this hydrogen bond is considerably more asymmetric than that between $Y_Z$ and D1-His190. Consequently, proton transfer in this hydrogen bond would be expected to take place more slowly than between $Y_Z$ and D1-His190.

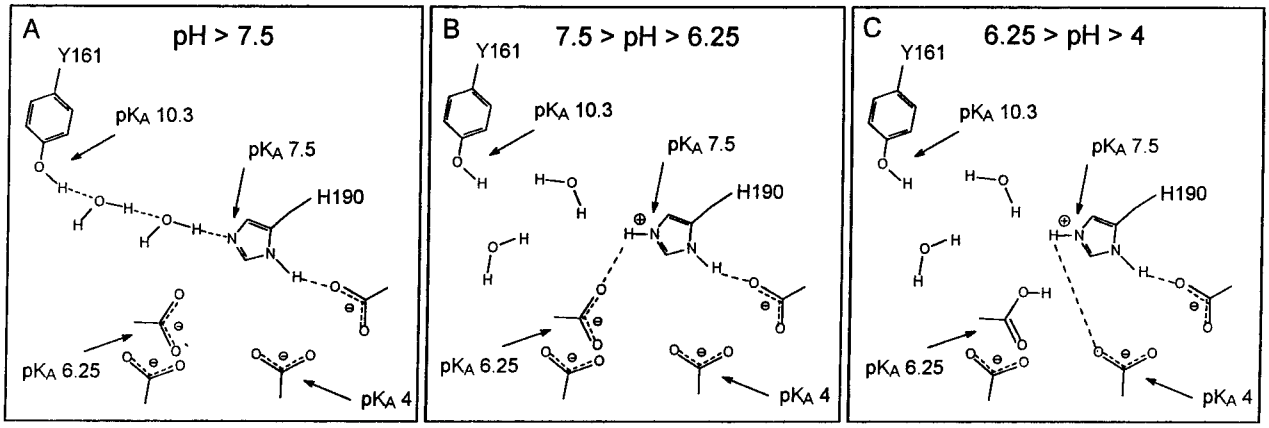


FIGURE 10: Proposed environment of $Y_Z$ (Y161) and D1-His190 in Mn-depleted wild-type* PSII particles. The apparent p$K_A$ values of $Y_Z$, D1-His190, and groups proposed to interact with D1-His190 are indicated. (Left panel) The deprotonation of $Y_Z$ is facilitated by the transient formation of a chain of hydrogen-bonded water molecules linking $Y_Z$ with D1-His190 ($k_1^{-1} = 0.25-0.7$ $\mu$s), in analogy to the situation in carbonic anhydrase (see text). (Center panel) The deprotonation of D1-His190 is facilitated by a hydrogen bond to a nearby group having p$K_A \approx 6.25$ (depicted as one of a pair of interacting carboxylate groups). (Right panel) The deprotonation of D1-His190 is facilitated by hydrogen bonds to one or more nearby groups having p$K_A \approx 4$.

bonded chain of at least two water molecules that transiently connects $Y_Z$ with D1-His190. This chain facilitates the deprotonation of $Y_Z$ and gives rise to $k_1$ (Figure 10A). An analogous situation is found in carbonic anhydrase, where the distance between the proton donor (His64) and the proton acceptor (a Zn-bound hydroxyl group) in the active site is ~8 Å (*107*−*110*). In this system, the overall activation energy for proton transfer is dominated by the energy required to properly orient the proton donor, the proton acceptor, and a hydrogen-bonded water chain that that transiently connects donor with acceptor (*108*, *110*−*114*). The actual rate-limiting step in this system may be proton transfer to the first water molecule in the transiently connected hydrogen-bonded water chain (*108*, *112*, *115*−*117*). This proton-transfer process has been described (*108*, *110*−*114*) in terms of Marcus proton transfer theory (*110*, *118*−*120*). In this theory, both the rate and the deuterium isotope effect for proton transfer show parabolic dependencies on the $\Delta pK_A$ between the proton donor and acceptor (*110*, *121*). The widths of these parabolic curves and the values of the rate constants and deuterium isotope effects at their maxima depend on the overall activation energy of the proton transfer reaction. For carbonic anhydrase, this includes the energy required to properly orient the hydrogen-bonded water chain. In Mn-depleted wild-type* PSII particles, the overall activation energy for proton transfer from $Y_Z$ to D1-His190, including the energy required to properly orient $Y_Z$, D1-His190, and a hydrogen-bonded water chain, would undoubtedly differ from that in the most thoroughly analyzed mutant of carbonic anhydrase (*108*, *110*, *111*). However, if the activation and reorientation energies in this mutant were the same as those in Mn-depleted wild-type* PSII particles, then the difference in p$K_A$ values between $Y_Z$ and D1-His190 ($pH_{acceptor}$ minus $pH_{donor} \approx -2.8$) would yield a deuterium isotope effect of ~2.1 (*110*, *111*) (see Figure 4 of ref *111*). Our value of $1.7 \pm 0.2$ for $k_1$ is consistent with this analysis.

Model B is consistent with the ENDOR data at all temperatures. This model would be consistent with the FTIR data (*91*) if $Y_Z$ forms a hydrogen bond with a water molecule in a majority of reaction centers, rather than with histidine. However, this interpretation conflicts with that offered in ref *91*.

It should be possible to discriminate between models A and B by performing a detailed proton inventory analysis on the rate of $P_{680}^{\bullet+}$ reduction measured in mixtures of $H_2O$ and $D_2O$ (*53*, *122*, *123*). Such an analysis reveals the number of protons involved in the transition state. The rate of $P_{680}^{\bullet+}$ reduction would be plotted as a function of the atom fraction of deuterium in solution. If proton transfer from $Y_Z$ to D1-His190 is direct, involving the movement of a single proton in the transition state (model A), then this plot will be linear. If proton transfer takes place via a hydrogen-bonded water chain, involving the movement of two or more protons in the transition state (model B), then this plot will bulge downward. In carbonic anhydrase, a proton inventory analysis ruled out direct proton transfer between His64 and the Zn-bound hydroxide and supported mechanisms involving a hydrogen-bonded chain of water molecules (*124*; also see refs *112* and *125*).

In both models, the oxidation of $Y_Z$ requires the reorientation of water molecules and/or amino acid side chains. These reorientations could account for the large activation energy for $Y_Z$ oxidation measured in Mn-depleted PSII preparations (*39*, *87*, *96*) compared to that measured in intact PSII preparations (*83*). Indeed, $Y_Z$ oxidation is "frozen out" at ~250 K in Mn-depleted PSII preparations (*96*), whereas $Y_Z$ oxidation occurs at temperatures as low as ~100 K in intact PSII preparations, at least during the $S_1 \rightarrow S_2$ transition (*126*, *127*). A "freezing out" of the proton-coupled electron-transfer reactions of $Y_Z$ at ~250 K would be consistent with charge recombination between $Q_A^{\bullet-}$ and $Y_Z^{\bullet}$ being the source of the thermoluminescence $A_T$ band in Mn-depleted PSII preparations, as discussed previously (*105*; G. W. Brudvig, personal communication]. The thermoluminescence $A_T$ band forms maximally at ~250 K (*128*) (for review of the controversy surrounding the origin of the $A_T$ band, see refs *3* and *129*).

*(3) Slower Phases of $P_{680}^{\bullet+}$ Reduction.* In intact PSII preparations, the microsecond phases of $P_{680}^{\bullet+}$ reduction exhibit significant deuterium isotope effects (*42*, *130*). The

relative amplitudes of these phases increase markedly below pH 6 and the half-time of one phase increased from ~5 $\mu$s at pH 6 to 30−40 $\mu$s at pH 4.5 (*82*). These phases have been postulated to represent either (i) relaxation processes involving proton movements that shift the equilibrium, $P_{680}^{\bullet+}$ $Y_Z$ ↔ $P_{680}$ $Y_Z^{\bullet}$, further to the right (*42*, *89*, *130*) or (ii) rate-limiting deprotonation events in proton pathways branching from D1-His190 (*58*). In the former model, the relaxation processes take place in all reaction centers and correspond to rearrangements of a hydrogen bond network that includes $Y_Z$ and D1-His190 (*89*). In the latter model, the deprotonation events occur in a fraction of reaction centers: those with proton pathways whose protonation states at the time of the actinic flash are suboptimal for rapid proton transfer from D1-His190 to the lumenal surface of PSII (*58*). These protonation states are likely to equilibrate with the lumen on a much slower time-scale than the nanosecond phases of $P_{680}^{\bullet+}$ reduction (*58*) because protonation/deprotonation events at the protein/water interface generally take place in microseconds or slower (*101*, *131*). Below pH 5, $P_{680}^{\bullet+}$ is reduced by $Q_A^{\bullet-}$ in a significant fraction of intact PSII reaction centers (*82*, *84*, *89*). This apparent inhibition of $Y_Z$ oxidation below pH 5 in intact PSII preparations has recently been attributed to the protonation of D1-His190 (*89*).

The relaxation processes (*42*, *89*, *130*) and proton-transfer pathways (*58*) that are postulated to exist in intact PSII preparations may also exist in Mn-depleted PSII preparations. Therefore, the slower phases of $P_{680}^{\bullet+}$ reduction in Mn-depleted wild-type* PSII particles (e.g., $k_2$ and $k_3$) may represent relaxation processes or deprotonation events far from $Y_Z$. However, if D1-His190 has p$K_A \approx 7.5$ (vide supra), it seems likely that $k_2$ and $k_3$ represent $Y_Z$ oxidation that is rate limited by the deprotonation of D1-His190 when this residue is protonated at the time of the actinic flash. The amplitudes of $k_2$ and $k_3$ appear to be inversely correlated (Figure 4, panels B and C) and the pH dependence of the amplitude of $k_3$ could be fit with a single proton titration curve having p$K_A \approx 6.25$ (Figure 4C). Therefore, the protonation state of a single residue may differentiate $k_2$ from $k_3$. One possibility is that the protonated form of D1-His190 forms a weak hydrogen bond to a nearby group having p$K_A \approx 6.25$ (depicted as one of a pair of interacting carboxylate residues in Figure 10B). This hydrogen bond could facilitate $Y_Z$ oxidation by facilitating the deprotonation of D1-His190. In this model, the rate of $Y_Z$ oxidation would be determined by $k_1$ and the ratio of the acid dissociation constants of D1-His190 and the nearby group, so that $k_2 = k_1 \times 10^{\Delta pK_A}/(1 + 10^{\Delta pK_A}) \approx k_1 \times 10^{\Delta pK_A}$, where $\Delta pK_A = (6.25-7.5)$. This relationship holds within a factor of 2 at pH values where both $k_1$ and $k_2$ were measured with the greatest accuracy (pH 7−8, Figure 5). At lower pH values, when the group having p$K_A \approx 6.25$ is protonated, D1-His190 may form weak hydrogen bonds to other groups having p$K_A < 4.5$ (Figure 10C). These hydrogen bonds may also facilitate the deprotonation of D1-His190, giving rise to $k_3$. The protonation of these groups may effectively block the oxidation of $Y_Z$ by $P_{680}^{\bullet+}$, so that the latter is reduced by $Q_A^{\bullet-}$ in a majority of reaction centers at pH ≤4.

Both Junge and co-workers (*39*) and Styring and co-workers (*34*) reported that $P_{680}^{\bullet+}$ was reduced by $Q_A^{\bullet-}$ in significant percentages of Mn-depleted reaction centers at pH <5.5. In contrast, we observed a third rapidly decaying phase ($k_3$, with $k_3^{-1} = 20-40$ $\mu$s), present maximally at pH ~5 (Figure 4C), that we attribute to $Y_Z$ oxidation in a fraction of reaction centers. One possible explanation is that, in *Chlamydomonas* and pea, the group having p$K_A$ ~6.25, postulated to exist in the previous paragraph, is not present or is positioned unfavorably with respect to influencing $P_{680}^{\bullet+}$ reduction. Perhaps this group is one of a pair of carboxylate residues that interact strongly in *Synechocystis* to raise one of their p$K_A$ values (e.g., see the appendix of ref *132*) but that do not interact strongly in *Chlamydomonas* or pea.[6]

*(4) Exogenous Organic Bases*. The slower components of $P_{680}^{\bullet+}$ reduction (e.g., $k_3$ and $k_4$) vanished in the presence of exogenous organic bases (Figure 1 and panels E and F of Figure 6). Imidazole, 1-methylimidazole, and histidine accelerated $P_{680}^{\bullet+}$ reduction by increasing the amplitude of $k_2$ at the expense of $k_3$ and $k_4$, whereas Tris increased the amplitude of $k_1$. Perhaps low concentrations of Tris facilitate the deprotonation of $Y_Z$ directly, whereas low concentrations of the other bases facilitate mainly the deprotonation of D1-His190. Imidazole, 1-methylimidazole, histidine, and Tris exhibited half-saturation values of ~4, ~4, <1, and ~7 mM respectively (Figure 1 and panels D−F of Figure 6). One possibility is that these represent the $K_D$ values for these bases binding in the vicinity of D1-His190 or $Y_Z$. However, an alternate possibility is that these bases reach D1-His190 or $Y_Z$ via a small-diameter channel and that the passage of exogenous bases through this channel is rate-limited by the reorientation of one or more amino acid side chains. This type of "gated entry" was suggested to govern the access of most exogenous bases to $Y_Z$ in D1-His190 mutants (*35*) and is believed to govern the incorporation of $Cu^{2+}$ into apoplastocyanin (*136*) and apo-azurin (*137*). In these proteins, the entry of $Cu^{2+}$ into its binding site is believed to be rate limited by the reorientation of a specific histidine residue. The rate of entry shows a hyperbolic dependence on $Cu^{2+}$ concentration that involves rapid binding of $Cu^{2+}$ to the apoprotein followed by the rate-limiting conformational change that permits entry into the $Cu^{2+}$ site (*138*).

## CONCLUDING REMARKS

We conclude that the hydrogen bond between $Y_Z$ and D1-His190 (*41*, *58*, *89*) is disrupted in the absence of the Mn cluster. A similar disruption of hydrogen bonding between $Y_Z$ and D1-His190 may occur in samples depleted of $Ca^{2+}$ (*139*, *140*) or treated with high concentrations of acetate (*141*, *142*). Both treatments dramatically slow the oxidation of $Y_Z$ by $P_{680}^{\bullet+}$. In the absence of the Mn cluster, the oxidation of $Y_Z$ either occurs as a concerted electron/proton-transfer event or is rate limited by the deprotonation of $Y_Z$. In either case, the rate-limiting step may involve the transient formation of a hydrogen bond or a hydrogen-bonded water bridge between $Y_Z$ and D1-His190. The slower phases of $P_{680}^{\bullet+}$ reduction (e.g., $k_2$ and $k_3$) probably correspond to the deprotonation of D1-His190 in reaction centers having this residue protonated at the time of the actinic flash. As a simple model, D1-His190 is proposed to interact with nearby residues having p$K_A$ values near 6 and 4. Because $Y_Z$ is located near the Mn

[6] Complex titration behavior for multiple interacting carboxylic acid residues has been predicted (*74*, *75*) and observed (*133*−*135*) in reaction centers from *Rhodobacter sphaeroides*.

cluster (*14*−*16*), these residues may ligate the Mn cluster in intact PSII preparations. The identity of these residues, and the residue that may accept a hydrogen bond from the $\delta$1 nitrogen of D1-His190, might be determined by analyzing the pH dependence of $P_{680}^{\bullet+}$ reduction in PSII particles isolated from site-directed mutants. These residues may be among those predicted to be near $Y_Z$ in recent modeling studies (*26*−*29*) or shown to influence the Mn cluster in site-directed mutagenesis studies (e.g., refs *33*, *43*, and *143*−*147*). Such residues include D1-Gln165, D1-Asp170, D1-Glu189, D1-His332, D1-Glu333, D1-His337, and D1-Asp342.

## ACKNOWLEDGMENT

We are grateful to J. Biggins for the gift of the semiconductor diode laser, to G. T. Babcock and C. Tommos for providing a preprint of ref *58*, to G. T. Babcock (especially), C. Berthomieu, G. W. Brudvig, R. D. Britt, K. A. Campbell, B. A. Diner, M. F. Dunn, M. Y. Okamura, M. L. Paddock, D. N. Silverman, S. Styring, B. Svensson, and W. Junge for many stimulating discussions, and to A. P. Nguyen for maintaining the wild-type* and mutant cultures of *Synechocystis* 6803. Finally, we thank G. T. Babcock, G. W. Brudvig, and B. A. Diner for critical comments on the manuscript.

## REFERENCES

1. Rhee, K. H., Morris, E. P., Barber, J., and Kühlbrandt, W. (1998) *Nature 396*, 283−286.
2. Hankamer, B., Morris, E. P., and Barber, J. (1999) *Nat. Struct. Biol. 6*, 560−564.
3. Debus, R. J. (1992) *Biochim. Biophys. Acta 1102*, 269−352.
4. Britt, R. D. (1996) in *Oxygenic Photosynthesis: The Light Reactions* (Ort, D. R., and Yocum, C. F., Eds.) pp 137−164, Kluwer Academic Publishers, Dordrecht, The Netherlands.
5. Diner, B. A., and Babcock, G. T. (1996) in *Oxygenic Photosynthesis: The Light Reactions* (Ort, D. R., and Yocum, C. F., Eds.) pp 213−247, Kluwer Academic Publishers, Dordrecht, The Netherlands.
6. Yachandra, V. K., Sauer, K., and Klein, M. P. (1996) *Chem. Rev. 96*, 2927−2950.
7. Renger, G. (1997) *Physiol. Plant. 100*, 828−841.
8. Penner-Hahn, J. E. (1998) *Struct. Bonding 90*, 1−36.
9. Hoganson, C. W., and Babcock, G. T. (1999) Manganese and Its Role in Biological Processes. In *Metal Ions in Biological Systems* (Sigel, A., and Sigel, H., Eds.) Vol. 37, pp 613−656, Marcel Dekker, New York.
10. Debus, R. J. (1999) Manganese and Its Role in Biological Processes. In *Metal Ions in Biological Systems* (Sigel, A., and Sigel, H., Eds.) Vol. 37, pp 657−710, Marcel Dekker, New York.
11. Roelofs, T. A., Liang, W., Latimer, M. J., Cinco, R. M., Rompel, A., Andrews, J. C., Sauer, K., Yachandra, V. K., and Klein, M. P. (1996) *Proc. Natl. Acad. Sci. U.S.A. 93*, 3335−3340.
12. Iuzzolino, L., Dittmer, J., Dörner, W., Meyer-Klaucke, W., and Dau, H. (1998) *Biochemistry 37*, 17112−17119.
13. Koulougliotis, D., Tang, X.-S., Diner, B. A., and Brudvig, G. W. (1995) *Biochemistry 34*, 2850−2856.
14. Peloquin, J. M., Campbell, K. A., and Britt, R. D. (1998) *J. Am. Chem. Soc. 120*, 6840−6841.
15. Dorlet, P., Di Valentin, M., Babcock, G. T., and McCracken, J. L. (1998) *J. Phys. Chem. B 102*, 8239−8247.
16. Lakshmi, K. V., Eaton, S. S., Eaton, G. R., Frank, H. A., and Brudvig, G. W. (1998) *J. Phys. Chem. B 102*, 8327−8335.
17. Limburg, J., Szalai, V. A., and Brudvig, G. W. (1999) *J. Chem. Soc., Dalton Trans.* 1353−1361.
18. Tommos, C., Tang, X.-S., Warncke, K., Hoganson, C. W., Styring, S., McCracken, J., Diner, B. A., and Babcock, G. T. (1995) *J. Am. Chem. Soc. 117*, 10325−10335.
19. Hoganson, C. W., Lydakis-Simantiris, N., Tang, X.-S., Tommos, C., Warncke, K., Babcock, G. T., Diner, B. A., McCracken, J., and Styring, S. (1995) *Photosynth. Res. 46*, 177−184.
20. Gilchrist, M. L., Jr., Ball, J. A., Randall, D. W., and Britt, R. D. (1995) *Proc. Natl. Acad. Sci. U.S.A. 92*, 9545−9549.
21. Babcock, G. T. (1995) in *Photosynthesis: From Light to Biosphere* (Mathis, P., Ed.) Vol. II, pp 209−215, Kluwer Academic Publishers, Dordrecht, The Netherlands.
22. Hoganson, C. W., and Babcock, G. T. (1997) *Science 277*, 1953−1956.
23. Tommos, C., and Babcock, G. T. (1998) *Acc. Chem. Res. 31*, 18−25.
24. Tommos, C., Hoganson, C. W., Di Valentin, M., Lydakis-Simantiris, N., Dorlet, P., Westphal, K., Chu, H.-A., McCracken, J., and Babcock, G. T. (1998) *Curr. Opin. Chem. Biol. 2*, 244−252.
25. Haumann, M., and Junge, W. (1999) *Biochim. Biophys. Acta 1411*, 86−91.
26. Svensson, B., Vass, I., Cedergren, E., and Styring, S. (1990) *EMBO J. 9*, 2051−2059.
27. Ruffle, S. V., Donnelly, D., Blundell, T. L., and Nugent, J. H. A. (1992) *Photosynth. Res. 34*, 287−300.
28. Svensson, B., Etchebest, C., Tuffery, P., Van Kan, P., Smith, J., and Styring, S. (1996) *Biochemistry 35*, 14486−14502.
29. Xiong, J., Subramaniam, S., and Govindjee (1998) *Photosynth. Res. 56*, 229−254.
30. Diner, B. A., Nixon, P. J., and Farchaus, J. W. (1991) *Curr. Opin. Struct. Biol. 1*, 546−554.
31. Roffey, R. A., Kramer, D. M., Govindjee, and Sayre, R. T. (1994) *Biochim. Biophys. Acta 1185*, 257−270.
32. Roffey, R. A., van Wijk, K. J., Sayre, R. T., and Styring, S. (1994) *J. Biol. Chem. 269*, 5115−5121.
33. Chu, H.-A., Nguyen, A. P., and Debus, R. J. (1995) *Biochemistry 34*, 5839−5858.
34. Mamedov, F., Sayre, R. T., and Styring, S. (1998) *Biochemistry 37*, 14245−14256.
35. Hays, A.-M. A., Vassiliev, I. R., Golbeck, J. H., and Debus, R. J. (1998) *Biochemistry 37*, 11352−11365.
36. Diner, B. A., and Nixon, P. J. (1998) in *Photosynthesis: Mechanisms and Effects* (Garab, G., Ed.) Vol. II, pp 1177−1180, Kluwer Academic Publishers, Dordrecht, The Netherlands.
37. Christen, G., Karge, M., Eckert, H.-J., and Renger, G. (1997) *Photosynthetica 33*, 529−539.
38. Haumann, M., Bögershausen, O., Cherepanov, D., Ahlbrink, R., and Junge, W. (1997) *Photosynth. Res. 51*, 193−208.
39. Ahlbrink, R., Haumann, M., Cherepanov, D., Bögershausen, O., Mulkidjanian, A., and Junge, W. (1998) *Biochemistry 37*, 1131−1142.
40. Diner, B. A., Force, D. A., Randall, D. W., and Britt, R. D. (1998) *Biochemistry 37*, 17931−17943.
41. Karge, M., Irrgang, K.-D., Sellin, S., Feinäugle, R., Liu, B., Eckert, H.-J., Eichler, H. J., and Renger, G. (1996) *FEBS Lett. 378*, 140−144.
42. Schilstra, M. J., Rappaport, F., Nugent, J. H. A., Barnett, C. J., and Klug, D. R. (1998) *Biochemistry 37*, 3974−3981.
43. Chu, H.-A., Nguyen, A. P., and Debus, R. J. (1994) *Biochemistry 33*, 6137−6149.
44. Chu, H.-A., Nguyen, A. P., and Debus, R. J. (1995) in *Photosynthesis: From Light to Biosphere* (Mathis, P., Ed.) Vol. II, pp 439−442, Kluwer Academic Publishers, Dordrecht, The Netherlands.
45. Vermaas, W. F. J. (1994) *Biochim. Biophys. Acta 1187*, 181−186.
46. Debus, R. J., Barry, B. A., Babcock, G. T., and McIntosh, L. (1988) *Proc. Natl. Acad. Sci. U.S.A. 85*, 427−430.
47. Tang, X.-S., and Diner, B. A. (1994) *Biochemistry 33*, 4594−4603.
48. Vassiliev, I. R., Jung, Y. S., Mamedov, M. D., Semenov, A. Y., and Golbeck, J. H. (1997) *Biophys. J. 72*, 301−315.

49. Glasoe, P. K., and Long, F. A. (1960) *J. Phys. Chem. 64*, 188−191.
50. Salomaa, P., Schaleger, L. L., and Long, F. A. (1964) *J. Am. Chem. Soc. 86*, 1−7.
51. Mathis, P., and Sétif, P. (1981) *Isr. J. Chem. 21*, 316−320.
52. Schowen, K. B., and Schowen, R. L. (1982) *Methods Enzymol. 87*, 551−606.
53. Quinn, D. M., and Sutton, L. D. (1991) in *Enzyme Mechanism from Isotope Effects* (Cook, P. F., Ed.) pp 73−126, CRC Press, Boca Raton, FL.
54. Vermaas, W. F. J., Rutherford, A. W., and Hansson, Ö. (1988) *Proc. Natl. Acad. Sci. U.S.A. 85*, 8477−8481.
55. Debus, R. J., Barry, B. A., Sithole, I., Babcock, G. T., and McIntosh, L. (1988) *Biochemistry 27*, 9071−9074.
56. Metz, J. G., Nixon, P. J., Rögner, M., Brudvig, G. W., and Diner, B. A. (1989) *Biochemistry 28*, 6960−6969.
57. Graige, M. S., Paddock, M. L., Bruce, J. M., Feher, G., and Okamura, M. Y. (1996) *J. Am. Chem. Soc. 118*, 9005−9016.
58. Tommos, C., and Babcock, G. T. (1999) *Biochim. Biophys. Acta* (in press).
59. Klimov, V. V., Allakhverdiev, S. I., Demeter, S., and Krasnovsky, A. A. (1979) *Dokl. Akad. Nauk SSSR 249*, 227−230.
60. Schweitzer, R. H., and Brudvig, G. W. (1997) *Biochemistry 36*, 11351−11359.
61. Schweitzer, R. H., Melkozernov, A. N., Blankenship, R. E., and Brudvig, G. W. (1998) *J. Phys. Chem. B 102*, 8320−8326.
62. Babcock, G. T., and Sauer, K. (1975) *Biochim. Biophys. Acta 396*, 48−62.
63. Yerkes, C. T., and Babcock, G. T. (1980) *Biochim. Biophys. Acta 590*, 360−372.
64. Ghanotakis, D. F., Yerkes, C. T., and Babcock, G. T. (1982) *Biochim. Biophys. Acta 682*, 21−31.
65. Babcock, G. T., Ghanotakis, D. F., Ke, B., and Diner, B. A. (1983) *Biochim. Biophys. Acta 723*, 276−286.
66. Tommos, C., McCracken, J., Styring, S., and Babcock, G. T. (1998) *J. Am. Chem. Soc. 120*, 10441−10452.
67. Bradbury, J. H., and Carver, J. A. (1984) *Biochemistry 23*, 4905−4913.
68. Anderson, D. E., Becktel, W. J., and Dahlquist, F. W. (1990) *Biochemistry 29*, 2403−2408.
69. Sprang, S., Standing, T., Fletterick, R. J., Stroud, R. M., Finer-Moore, J., Xuong, N.-H., Hamlin, R., Rutter, W. J., and Craik, C. S. (1987) *Science 237*, 905−909.
70. Craik, C. S., Roczniak, S., Largman, C., and Rutter, W. J. (1987) *Science 237*, 909−913.
71. Christianson, D. W., and Alexander, R. S. (1989) *J. Am. Chem. Soc. 111*, 6412−6419.
72. Goodin, D. B., and McRee, D. E. (1993) *Biochemistry 32*, 3313−3324.
73. Sternberg, M. J. E., Hayes, F. R. F., Russell, A. J., Thomas, P. G., and Fersht, A. R. (1987) *Nature 330*, 86−88.
74. Gunner, M. R., and Honig, B. (1992) in *The Photosynthetic Bacterial Reaction Center II* (Breton, J., and Verméglio, A., Eds.) pp 403−410, Plenum Press, New York.
75. Beroza, P., Fredkin, D. R., Okamura, M. Y., and Feher, G. (1995) *Biophys. J. 68*, 2233−2250.
76. Creighton, T. E. (1993) *Proteins: Structures and Molecular Properties*, W. H. Freeman and Company, New York.
77. Haumann, M., Mulkidjanian, A., and Junge, W. (1999) *Biochemistry 38*, 1258−1267.
78. Pin, S., Alpert, B., Cortès, R., Ascone, I., Chiu, M. L., and Sligar, S. G. (1994) *Biochemistry 33*, 11618−11623.
79. Tang, H.-L., Chance, B., Mauk, A. G., Powers, L. S., Reddy, K. S., and Smith, M. (1994) *Biochim. Biophys. Acta 1206*, 90−96.
80. Brettel, K., Schlodder, E., and Witt, H. T. (1984) *Biochim. Biophys. Acta 766*, 403−415.
81. Schlodder, E., Brettel, K., and Witt, H. T. (1985) *Biochim. Biophys. Acta 808*, 123−131.
82. Schlodder, E., and Meyer, B. (1987) *Biochim. Biophys. Acta 890*, 23−31.
83. Eckert, H.-J., and Renger, G. (1988) *FEBS Lett. 236*, 425−431.
84. Meyer, B., Schlodder, E., Dekker, J. P., and Witt, H. T. (1989) *Biochim. Biophys. Acta 974*, 36−43.
85. Lukins, P. B., Post, A., Walker, P. J., and Larkum, A. W. D. (1996) *Photosynth. Res. 49*, 209−221.
86. Christen, G., Reifarth, F., and Renger, G. (1998) *FEBS Lett. 429*, 49−52.
87. Renger, G., Christen, G., Karge, M., Eckert, H.-J., and Irrgang, K.-D. (1998) *J. Biol. Inorg. Chem. 3*, 360−366.
88. Candeias, L. P., Turconi, S., and Nugent, J. H. A. (1998) *Biochim. Biophys. Acta 1363*, 1−5.
89. Christen, G., Seeliger, A. G., and Renger, G. (1999) *Biochemistry 38*, 6082−6092.
90. Noguchi, T., Inoue, Y., and Tang, X. S. (1997) *Biochemistry 36*, 14705−14711.
91. Berthomieu, C., Hienerwadel, R., Boussac, A., Breton, J., and Diner, B. A. (1998) *Biochemistry 37*, 10547−10554.
92. Szczesniak, M. M., and Scheiner, S. (1985) *J. Phys. Chem. 89*, 1835−1840.
93. Scheiner, S. (1985) *Acc. Chem. Res. 18*, 174−180.
94. O'Malley, P. J. (1998) *J. Am. Chem. Soc. 120*, 11732−11737.
95. Conjeaud, H., Mathis, P., and Paillotin, G. (1979) *Biochim. Biophys. Acta 546*, 280−291.
96. Reinman, S., and Mathis, P. (1981) *Biochim. Biophys. Acta 635*, 249−258.
97. Reinman, S., Mathis, P., Conjeaud, H., and Stewart, A. (1981) *Biochim. Biophys. Acta 635*, 429−433.
98. Conjeaud, H., and Mathis, P. (1986) *Biophys. J. 49*, 1215−1221.
99. Scheiner, S. (1986) *Methods Enzymol. 127*, 456−465.
100. Scheiner, S. (1992) in *Proton Transfer in Hydrogen-Bonded Systems* (Bountis, T., Ed.) pp 29−47, Plenum Press, New York.
101. Gutman, M., and Nachliel, E. (1990) *Biochim. Biophys. Acta 1015*, 391−414.
102. Scheiner, S. (1994) *Acc. Chem. Res. 27*, 402−408.
103. Scheiner, S., and Latajka, Z. (1987) *J. Phys. Chem. 91*, 724−730.
104. Force, D. A., Randall, D. W., Britt, R. D., Tang, X.-S., and Diner, B. A. (1995) *J. Am. Chem. Soc. 117*, 12643−12644.
105. Tang, X.-S., Zheng, M., Chisholm, D. A., Dismukes, G. C., and Diner, B. A. (1996) *Biochemistry 35*, 1475−1484.
106. Un, S., Tang, X.-S., and Diner, B. A. (1996) *Biochemistry 35*, 679−684.
107. Silverman, D. N., and Lindskog, S. (1988) *Acc. Chem. Res. 21*, 30−36.
108. Silverman, D. N. (1995) *Methods Enzymol. 249*, 479−503.
109. Christianson, D. W., and Fierke, C. A. (1996) *Acc. Chem. Res. 29*, 331−339.
110. Kresge, A. J., and Silverman, D. N. (1999) *Methods Enzymol. 308* (in press).
111. Silverman, D. N., Tu, C., Chen, X., Tanhauser, S. M., Kresge, J., and Laipis, P. J. (1993) *Biochemistry 32*, 10757−10762.
112. Taoka, S., Tu, C., Kistler, K. A., and Silverman, D. N. (1994) *J. Biol. Chem. 269*, 17988−17992.
113. Ren, X., Tu, C., Laipis, P. J., and Silverman, D. N. (1995) *Biochemistry 34*, 8492−8498.
114. Tu, C., Qian, M., Earnhardt, J. N., Laipis, P. J., and Silverman, D. N. (1998) *Biophys. J. 74*, 3182−3189.
115. Liang, J.-Y., and Lipscomb, W. N. (1988) *Biochemistry 27*, 8676−8682.
116. Åqvist, J., and Warshel, A. (1992) *J. Mol. Biol. 224*, 7−14.
117. Toba, S., Colombo, G., and Merz, K. M., Jr. (1999) *J. Am. Chem. Soc. 121*, 2290−2302.
118. Marcus, R. A. (1968) *J. Phys. Chem. 72*, 891−899.
119. Cohen, A. O., and Marcus, R. A. (1968) *J. Phys. Chem. 72*, 4249−4256.
120. Kresge, A. J. (1975) *Acc. Chem. Res. 8*, 354−360.
121. Kresge, A. J., Sagatys, D. S., and Chen, H. L. (1977) *J. Am. Chem. Soc. 99*, 7228−7233.
122. Schowen, K. B. J. (1978) in *Transition States of Biochemical Processes* (Gandour, R. D., and Schowen, R. L., Eds.) pp 225−283, Plenum Press, New York.
123. Venkatasubban, K. S., and Schowen, R. L. (1984) *CRC Crit. Rev. Biochem. 17*, 1−44.

124. Venkatasubban, K. S., and Silverman, D. N. (1980) *Biochemistry 19*, 4984−4989.
125. Tu, C., and Silverman, D. N. (1982) *Biochemistry 21*, 6353−6360.
126. de Paula, J. C., Innes, J. B., and Brudvig, G. W. (1985) *Biochemistry 24*, 8114−8120.
127. Styring, S., and Rutherford, A. W. (1988) *Biochim. Biophys. Acta 933*, 378−387.
128. Koike, H., Siderer, Y., Ono, T.-A., and Inoue, Y. (1986) *Biochim. Biophys. Acta 850*, 80−89.
129. Kramer, D. M., Roffey, R. A., Govindjee, and Sayre, R. T. (1994) *Biochim. Biophys. Acta 1185*, 228−237.
130. Christen, G., and Renger, G. (1999) *Biochemistry 38*, 2068−2077.
131. Gutman, M., and Nachliel, E. (1995) *Biochim. Biophys. Acta 1231*, 123−138.
132. Paddock, M. L., Rongey, S. H., McPherson, P. H., Juth, A., Feher, G., and Okamura, M. Y. (1994) *Biochemistry 33*, 734−745.
133. Hienerwadel, R., Grzybek, S., Fogel, C., Kreutz, W., Okamura, M. Y., Paddock, M. L., Breton, J., Nabedryk, E., and Mäntele, W. (1995) *Biochemistry 34*, 2832−2843.
134. Nabedryk, E., Breton, J., Hienerwadel, R., Fogel, C., Mäntele, W., Paddock, M. L., and Okamura, M. Y. (1995) *Biochemistry 34*, 14722−14732.
135. Nabedryk, E., Breton, J., Okamura, M. Y., and Paddock, M. L. (1998) *Biochemistry 37*, 14457−14462.
136. Garrett, T. P. J., Clingeleffer, D. J., Guss, J. M., Rogers, S. J., and Freeman, H. C. (1984) *J. Biol. Chem. 259*, 2822−2825.
137. Nar, H., Messerschmidt, A., Huber, M., van de Camp, M., and Canters, G. W. (1992) *FEBS Lett. 306*, 119−124.
138. Marks, R. H. L., and Miller, R. D. (1979) *Arch. Biochem. Biophys. 195*, 103−111.
139. Boussac, A., Sétif, P., and Rutherford, A. W. (1992) *Biochemistry 31*, 1224−1234.
140. Haumann, M., and Junge, W. (1999) *Biochim. Biophys. Acta 1411*, 121−133.
141. Saygin, Ö., Gerken, S., Meyer, B., and Witt, H. T. (1986) *Photosynth. Res. 9*, 71−78.
142. Gerken, S., Dekker, J. P., Schlodder, E., and Witt, H. T. (1989) *Biochim. Biophys. Acta 977*, 52−61.
143. Nixon, P. J., and Diner, B. A. (1992) *Biochemistry 31*, 942−948.
144. Boerner, R. J., Nguyen, A. P., Barry, B. A., and Debus, R. J. (1992) *Biochemistry 31*, 6660−6672.
145. Diner, B. A., and Nixon, P. J. (1992) *Biochim. Biophys. Acta 1101*, 134−138.
146. Nixon, P. J., and Diner, B. A. (1994) *Biochem. Soc. Trans. 22*, 338−343.
147. Chu, H.-A., Nguyen, A. P., and Debus, R. J. (1995) *Biochemistry 34*, 5859−5882.

BI990716A